Universidade de Aveiro Departamento de Biologia
2014

JOSÉ RUI LIMA PAITIO

Vision and behaviour in deep-sea fishes: distribution of neural retinal cells in Myctophidae

Visão e comportamento em peixes de profundidade: distribuição de células neurais da retina em Myctophidae

DECLARAÇÃO

Declaro que este relatório é integralmente da minha autoria, estando devidamente referenciadas as fontes e obras consultadas, bem como identificadas de modo claro as citações dessas obras. Não contém, por isso, qualquer tipo de plágio quer de textos publicados, qualquer que seja o meio dessa publicação, incluindo meios eletrónicos, quer de trabalhos académicos.

Universidade de Aveiro Departamento de Biologia
2014

JOSÉ RUI LIMA PAITIO

Vision and behaviour in deep-sea fishes: distribution of neural retinal cells in Myctophidae

Visão e comportamento em peixes de profundidade: distribuição de células neurais da retina em Myctophidae

Dissertação apresentada à Universidade de Aveiro para cumprimento dos requisitos necessários à obtenção do grau de Mestre em Biologia Marinha, realizada sob a orientação científica da Professora Doutora Maria Marina Pais Ribeiro da Cunha, Professor Auxiliar do Departamento de Biologia da Universidade de Aveiro

“Faz mais quem quer que quem pode.”

Ditado tradicional português

o júri

presidente

Prof. Doutor João António de Almeida Serôdio
Professor Auxiliar do Departamento de Biologia da Universidade de Aveiro

Doutora Fanny de Busserolles
Investigadora de Pós-doutoramento, *King Abdullah University of Science and Technology*

Prof.ª Doutora Maria Marina Pais Ribeiro da Cunha
Professora Auxiliar do Departamento de Biologia da Universidade de Aveiro

agradecimentos

Antes de mais, gostaria de agradecer a todos os que contribuíram para este trabalho e que, eventualmente, vou-me esquecer de referir.
Primeiramente, aos meus pais, irmão, família e amigos, que desde sempre me apoiaram nesta saga.
À minha orientadora, Professora Marina Cunha, a quem devo a oportunidade de executar este trabalho e por todo o apoio, directrizes e disponibilidade ao longo do mesmo.
Ao Rui Vieira, o co-orientador "não-oficial" que o foi, por toda a ajuda, disponibilidade e, essencialmente, paciência para todas as dúvidas "parvas".
I wish to thank to Fanny de Busserolles, *for her availability, comprehension and support in all questions during this study that was unknown to me before I started it.*
I would also like to thank to Ming-Tsung Chung *for his patience and availability to support me in methodological doubts, essentially.*
Agradeço à Ana Hilário a ajuda em dúvidas "existencio-laboratoriais" e por me fazer questionar a exequibilidade metodológica, levando à sua optimização.
Gostaria de agradecer também ao Fábio Matos, por auxiliar este "jumento estatístico" a conseguir executar algumas análises de dados.
Agradeço à Ascensão Ravara, Luciana Génio, Susana Oliveira e Clara Rodrigues pela disponibilidade em questões de logística laboratorial.
Não menos, tenho de agradecer em geral a todo o "pessoal do LEME!" por todo o apoio e boa-disposição. Obrigado ao Filipe Laranjeiro e à Mariana Almeida pelo apoio moral e paciência. Agradeço também às minhas "colegas" Diana Ramos, Inês Guedes e Joana Casais, pelas muitas horas de "pachorra" e apoio, em todo este ordálio que pode (não) ser uma tese de mestrado.

palavras-chave mar profundo, zona mesopelágica, Myctophidae, peixe-lanterna, visão, retina.

resumo

O objectivo deste trabalho centrou-se na análise das distribuições de densidade em células neuronais de retinas de mictofídeos e na relação com parâmetros ecológicos e comportamentais. *Retinal wholemounting technique* permitiu a determinação de densidades topográficas de fotoreceptores (PRs), células ganglionares da retina (RGCs) e células amácrinas (ACs) em mictofídeos adultos. Estes dados possibilitam a identificação de especializações retinais e desenvolver estimativas de acuidade e sensibilidade visual, assim como sensibilidade à luz de origem bioluminescente ou solar. As sete espécies de mictofídeos analisadas apresentam elevada densidade de PRs e baixas densidades de RGCs. Especializações retinais divergentes reflectem diferenças comportamentais entre espécies de mictofídeos. Os parâmetros visuais são influenciados essencialmente por factores ecológicos, mas as relações filogenéticas são também um factor que poderá explicar os padrões de distribuição de células retinais em mictofídeos. Concluindo, as espécies estudadas revelam elevada sensibilidade visual e baixa acuidade, sugerindo uma grande adaptação às condições de luminosidade da zona mesopelágica.

keywords deep-sea, mesopelagic zone, Myctophidae, lanternfish, vision, retina.

abstract

This work aims to analyse the density and distribution of neuron cells on retinae of myctophid fishes in relation to ecological and behavioural parameters. Retinal wholemounting technique allowed the observation of topographic densities for photoreceptors (PRs), retinal ganglion cells (RGCs) and amacrine cells (ACs) in adult myctophids. These data allowed the identification of retinal specializations and the estimation of visual acuity and sensitivity, and sensitivity to bioluminescence flashes and to downwelling light. The seven analysed myctophid species showed high density of PRs and low density for RGCs. Different retinal specializations reflect behavioural differences between myctophid species. Visual parameters are influenced mainly by ecological factors, but phylogenetic relationships are also a factor that may explain the distribution of retinal cells in myctophids. In conclusion, all species in this study showed high visual sensitivity and low acuity, suggesting a great adaptation to mesopelagic light conditions.

Table of contents

List of figures

List of tables

1. Introduction

The mesopelagic zone is the region in the water column between 200 and 1000 m depth, defined as the oceanic layer where sunlight penetration is insufficient for photosynthesis but allows the fauna to differentiate between day and night (Douglas *et al*., 1995; Turner *et al*., 2009; Robinson *et al*., 2010; Sutton, 2013). Known also as dysphotic or twilight zone, the mesopelagic layer represents the transition from the upwards epipelagic photic zone to the aphotic downwards bathypelagic zone (Salvanes & Kristoffersen, 2001; Robinson *et al*., 2010; Sutton, 2013). Although biophysical conditions become more stable over time and space in the mesopelagic zone, it presents a gradient in environmental parameters (Robinson *et al*., 2010; Sutton, 2013). Environmental conditions at mesopelagic depths are very particular, showing mainly dim light, cold waters with oxygen minimum levels, reduced turbulence, increased hydrostatic pressure, high inorganic nutrient concentrations and irregular food supply (Robinson *et al*., 2010; Catul *et al*., 2011). Mesopelagic zone may be split at 600-700 m depth as upper and lower mesopelagic (Warrant & Locket, 2004; Sutton, 2013). The upper mesopelagic is illuminated essentially by downwelling sunlight and its incidence on objects creates extended light scenes whilst lower mesopelagic is dominated by bioluminescent flashes, representing a different light scene with point source light (Wagner *et al*., 1998; Warrant & Locket, 2004; Yakir *et al*., 2013). The adaptation of deep-sea fishes to one or both light conditions varies interspecifically, depending on ecological drivers, environment (changing nature of visual scenes), and species-specific ecological traits (natural histories) (Warrant & Locket, 2004). Camouflage strategies change through the mesopelagic zone in relation to light source types and regimes. At the upper mesopelagic zone, fishes generally present silver coloration and large photophores, as an adaptation for predator avoidance in dim light, whilst at the lower mesopelagic zone, where light penetration is diminished, fishes are dark-coloured, from black to crimson (Warrant & Locket, 2004; Catul *et al*., 2011; Sutton, 2013).

At mesopelagic depths, sources of the available monochromatic and dim light (Fig. 1) are downwelling sunlight and bioluminescence (Douglas *et al*., 1995; Haddock *et al*., 2010; Johnsen, 2005; Lythgoe & Partridge, 1989). The downwelling light available corresponds only to a narrow blue-green bandwidth, with wavelength between 470-490 nm (Douglas *et al*., 1995; Turner *et al*., 2009).

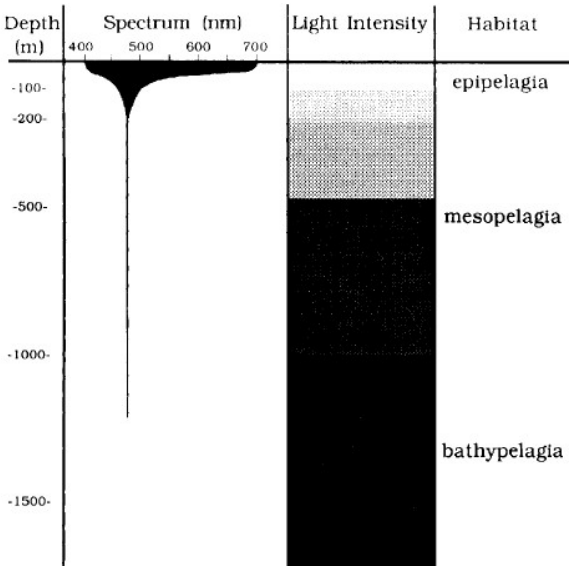

Figure 1 – Scheme of light spectra and intensity distributions along the oceanic depths and zones. From Evans & Fernald (1990).

Considering that about 80% of the deep-sea species are bioluminescent and the sunlight is scarcely penetrating down to these depths, bioluminescence is the most important light source to animals living in mesopelagic and deeper depths (Douglas *et al*., 1995; Douglas *et al*., 1998; Turner *et al*., 2009; Sutton, 2013). Bioluminescence light presents spectral emission maxima (λImax) of 450-520 nm (Partridge *et al*., 1989; Turner *et al*., 2009). Biological light production by mesopelagic fishes is used, for instance, for intraspecific identification and communication and interspecific purposes - attraction and identification of prey (Turner *et al*., 2009; Haddock *et al*., 2010). Bioluminescence is widely used for camouflage functions, mostly for counterillumination, where for instance prey's ventral photophores match the downwelling light disrupting their silhouettes for the downside viewer, the predator with monochromatic retinas (Cocker, 1978; Johnsen *et al*., 2004; Turner *et al*., 2009; Haddock *et al*., 2010). Other examples of the biological produced light function include lures to illuminate prey (e.g. the barbell of stomiids), luminous flashes, and smokescreen to startle or confuse predators (e.g., squids and crustaceans) (Cocker, 1978; Haddock *et al*., 2010).

Mesopelagic conditions influence distribution and behaviour of fauna, with remarkable behavioural, physiological and morphological adaptations (Robinson *et al*., 2010; Catul *et al*., 2011; Sutton, 2013). At these depths many animals retreat during daytime from visual predators ("anti-predator-window"), as many species, mostly from the upper mesopelagic zone, perform diel vertical migrations (DVM) (Salvanes & Kristoffersen, 2001; Robinson *et al*., 2010; Sutton, 2013).

DVM behaviour aims at feeding during the night at shallower depths while staying in relative inactivity at mesopelagic depths during daytime (Robinson *et al*., 2010; Sutton, 2013). DVM is a crucial process for energy exchange between lower and higher trophic levels and it also has an important contribution for the biological pump of organic carbon, nitrogen and phosphorus at deeper waters (Bergstad *et al*., 2003; Robinson *et al*., 2010). Over 90% of the organic carbon is vertically exported from epipelagic and turned back into carbon dioxide by mesopelagic communities from respiration, faecal pellets, predation and dissolved organic matter (Robinson *et al*., 2010).

As a dim scene of light changing conditions, essentially for DVM species, mesopelagic zone is a habitat where species with the most remarkable visual adaptations are found. Light sensitivity is crucial to fishes for DVM both for perceiving bioluminescent signals and for matching its own counterillumination to downwelling light (Robinson *et al*. 2010).

1.1. Vision of deep-sea fishes

In an environment where light has such an important ecological role, mesopelagic fishes rely mainly on the sense of vision (Cocker, 1978). In fact, mesopelagic fishes have an optic tectum more developed than other sensorial brain parts (Collin *et al*., 2000; Salvanes & Kristoffersen, 2001; Wagner, 2002), and in some cases (e.g. myctophids) the pineal organ presents an extraocular photoreceptor and is able to discriminate slow environmental light shifts (Young *et al*., 1979; Bowmaker & Wagner, 2004). Also, deep-sea fishes may be able to detect dim sunlight down to 1150 m depth (Denton & Warren, 1957). These fishes evolved in order to exceptionally adapt to the extreme environmental conditions, by developing sensitive monochromatic vision at dim light (O'Day & Fernandez, 1976; Pankhurst, 1987; Yokoyama & Yokoyama, 1996). The main ocular adaptations are: large eyes and pupils, with aphakic gap (Yokoyama & Yokoyama, 1996; Warrant & Locket, 2004; Turner *et al*., 2009; de Busserolles *et al,* 2014); shortwave lens (Douglas *et al*., 1995; Douglas *et al*., 1998); fovea (Wagner *et al*., 1998; Warrant & Locket, 2004); tapetum lucidum (O'Day & Fernandez, 1976; Pankhurst, 1987; de Busserolles *et al.,* 2014); multiple banks arrangement of the retina (Pankhurst, 1987; Wagner, 2002); pure-rod retina (O'Day & Fernandez, 1976; Pankhurst, 1987; de Busseroles *et al.,* 2014); high density of large photoreceptor cells (Denton & Warren, 1957; Pankhurst, 1987; Hope *et al*., 1997; Hunt *et al*., 2001; Sabatés *et al*., 2003); high photoreceptors-ganglion cells convergence ratio (McNulty, 1976; Locket, 1980; Wagner, 2002); large-sized retinal photoreceptor outer segments (Pankhurst, 1987; Partridge *et al*., 1989); and high concentration of single pigmented rhodopsin (O'Day & Fernandez, 1976; Cocker, 1978; Partridge *et al*., 1989; Hope *et al*., 1997; Hunt *et al*., 2001).

Larger eyes present larger pupils allowing maximization of light entering the eye and, consequently long visual range, higher visual sensitivity and acuity (Douglas *et al*., 1998; Warrant & Locket, 2004).

The aphakic gap is an "extension" of the pupil located between the lens and the iris, permitting the entrance of light from oblique angles without passing through the lens (Warrant & Locket, 2004; de Busserolles, 2013). Therefore, aphakic gaps allow higher visual sensitivity in detriment of acuity (Douglas *et al*., 1998; Warrant & Locket, 2004; de Busserolles, 2013). Two types of aphakic gaps are classified: rostral and circumlental. Rostral aphakic gaps focus frontal light on the temporal part of the retina, enhancing light projection onto this area, while the circumlental aphakic gap surrounds the entire lens, increasing light entrance from all directions (Warrant & Locket, 2004; de Busserolles, 2013).

Lenses are transparent structures, which grow continually through life, and refract the incident light, focusing an image on the retina (Douglas *et al*., 1998; Warrant & Locket, 2004). It allows greater visual acuity proportionally to the lens size, as focal length enhances with lenses' diameter (Collin & Pettigrew, 1989; Warrant & Locket, 2004).

Light enters the eye (Fig. 2A) through the pupil (conditioned by the aphakic gap, when present), refracted by the lens and focused on the retina (Warrant & Locket, 2004; de Busserolles, 2013). The retina receives the light of the surroundings and sends it through the optical nerve, as an electric signal to the animal's brain (Collin & Pettigrew, 1989; Wagner *et al*., 1998; Warrant & Locket, 2004; de Busserolles, 2013). The retina is a thin multi-layered tissue composed by different types of neurons (Fig. 2B) (O'Day & Fernandez, 1976; Wagner *et al*., 1998; de Busserolles, 2013). The retina's outer side (scleral) is composed by visual cells (photoreceptors (PRs)) that receive and translate the light information into an electrical signal (Wagner *et al*., 1998; Ullmann *et al*., 2011; de Busserolles, 2013). This electric impulse is transmitted synaptically through multi-layered interneurons (plexiform layer) to the retinal ganglion cells (RGCs) on the inner (vitreal) side (Wagner *et al*., 1998; de Busserolles, 2013).

Among different types of interneurons are the amacrine cells (ACs, Fig. 2D), regulating the information from the interneurons to the RGCs. Teleosts possess around 40 types of ACs, many of them with specific functions still unknown (Wagner *et al*., 1998; de Busserolles, 2013). Unlike from the other neuronal cells, RGCs (Fig. 2D) possesses axons composing the optic nerve, which are responsible to link the eyes to the brain, sending the electric signals with the perceived environment to the visual centres of the brain, where the electric impulses are interpreted as images (Wagner *et al*., 1998; Collin *et al*., 2000; Warrant & Locket, 2004; de Busserolles, 2013). As the fish grows, the retinal growing is accompanied by an increase of RGCs number, but the densities

tend to decrease (Pankhurst, 1987; Collin & Pettigrew, 1989). Different types of RGCs are specialised for different characteristics of the perceived image (e.g. colour, movement, and contrast) and processed by different brain areas (Wagner *et al*., 1998; de Busserolles, 2013).

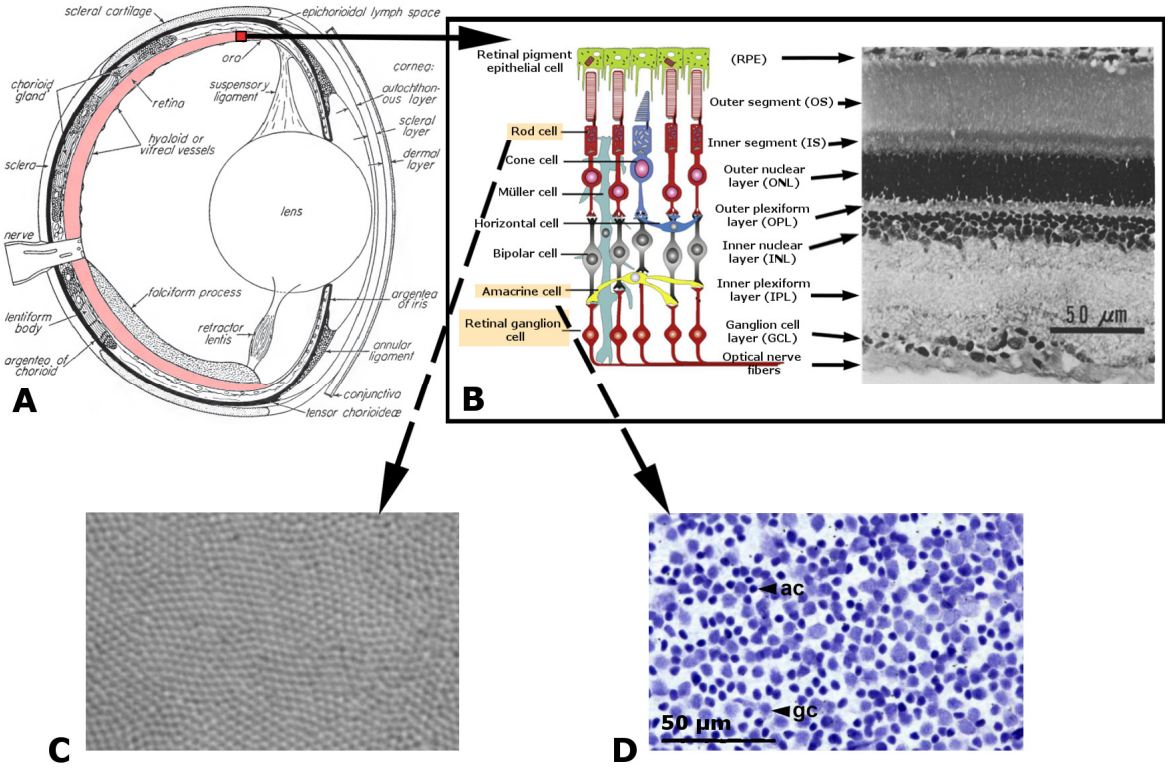

Figure 2 – Schematic representation of myctophids retinal structure. A) Vertical section of a teleost eye, highlighting the retina (adapted from de Busserolles (2103); B) Diagram and histological section of myctophid *Stenobrachius leucopsarus*, showing retinal cell types arrangement (modified from O'Day & Fernandez (1976) and de Busserolles (2013)); C) Wholemount view of the scleral side of a retina of *Myctophum brachygnatum* showing the PRs arrangement (adapted from de Busserolles (2103); D) Light microcraph of the vitreal side of a stained retina of *Ceratoscopelus warmingii* showing the retinal ganglion cells (GCs) and amacrine cells (ACs) disposition (adapted from de Busserolles (2103).

Photoreceptors are divided in two types: rods and cones (Fig. 2B) (Yokoyama & Yokoyama, 1996; Warrant & Locket, 2004; de Busserolles, 2013). Cones are linked to acute and coloured vision, and rods to light sensitivity, as they are hundred times more sensitive to light than cones (Partridge *et al*., 1988; Lythgoe & Partridge, 1989; Partridge *et al*., 1989; Yokoyama & Yokoyama, 1996; Douglas *et al*., 1998). Deep-sea fishes possess mostly pure-rod retinas (Fig. 2C) (Munk, 1977; Cocker, 1978; Lythgoe & Partridge, 1989). As rods detect a narrow interval of shortwaves they are linked to scotopic (nocturnal) monochromatic vision (Pankhurst, 1987; Partridge *et al*.,

1989; Yokoyama & Yokoyama, 1996; Warrant & Locket, 2004; Johnsen, 2005). The diameter of rods' outer segments are intra- and interspecific variable (Partridge *et al*., 1988; Partridge *et al*., 1989) and cell densities are constant or increase with fish age, as they have *in situ* origin from precursor cells mitosis (Locket, 1980). Multiple banks are photoreceptors arranged in multilayers, which may increase as the fish grows and photoreceptors may cover totally the retinal surface with visual pigment (Locket, 1980; Somiya, 1982).

The photoreceptors' outer segments (Fig. 2B) include the visual pigments, transforming the energy of the received photons into electrical signals (hyperpolarisation/transduction) and are responsible for visual sensitivity - retinal pigment maximum wavelength (λmax) absorption (Douglas *et al*., 1995; Turner *et al*., 2009; de Busserolles, 2013). These pigments are proteins – opsins – covalently bonded to a light absorbing chromophore, derived from vitamin A (Bowmaker *et al*., 1988; Yokoyama & Yokoyama, 1996; Hope *et al*., 1997; Hasegawa *et al*., 2008; Toyama *et al*., 2008). Most deep-sea fishes present rhodopsin, a pigment derived from vitamin A1, but some possess a chromophore derived from vitamin A2 (porphyropsin), which is more sensitive to longer wavelengths (Lythgoe & Partridge, 1989; Hasegawa *et al*., 2008; Toyama *et al*., 2008). Visual pigment is "tuned" by opsin, a chromophore and its interactions (Yokoyama & Yokoyama, 1996). Spectral information depends on the wavelengths of the photons reaching the photoreceptors and its retinal pigments (Denton *et al*., 1985; Bowmaker *et al*., 1988; Lythgoe & Partridge, 1989; Douglas *et al*., 1998). Deep-sea fishes present mainly single pigmented rhodopsin retinas as its λmax (470 - 500 nm) matches mesopelagic shortwave spectra (Denton & Warren, 1957; Lythgoe & Partridge, 1989; Douglas *et al*., 1998; Warrant & Locket, 2004). These shortwave pigments λmax are an adaptation to maximise signal, contrast and photon reception, and to reduce noise (Denton & Warren, 1957; Lythgoe & Partridge, 1989; Hope *et al*., 1997; Douglas *et al*., 1998). The pattern of amino acid residues of the opsin is responsible for the sensitivity of deep-sea fishes' rhodopsin to the dim light environment (Crescitelli *et al*., 1985; Hope *et al*., 1997; Douglas *et al*., 1998). On the other hand, Douglas *et al*. (1998) and Owens *et al*. (2012) suggest that deep-sea fishes show λmax phylogenetic conservatism along with the effect of ecological pressures, for instance, myctophid species have similar λmax despite inhabiting diverse depths and not all performing DVMs. Even so, these visual pigments and photoreceptors present in deep-sea fishes are an adaptation to light availability. Additionally, recent studies pointed to greater sensitivity to bioluminescence rather than to the downwelling light (Douglas *et al*., 1995; Douglas *et al*., 1998; Turner *et al*., 2009).

Fish retinas grow through life, adding new cells at the periphery, and therefore forcing the older cells towards the central area, but, as RGCs density decreases, retinal area for each cell information should increase with growth in order to keep a constant receptive field of constant visual angle

(Collin & Pettigrew, 1989). Retinal cells densities are not constant throughout the retina. In fact, cell topographic distributions reflect the animal's symmetry of the perceived environment (de Busserolles, 2013). The patterns of retinal cells reveal two main visual specializations (Fig. 3): area and horizontal streak (Collin & Pettigrew, 1989; Collin *et al*., 2000; de Busserolles, 2013). The area reflects concentric increases of cell densities and is linked to visual acuity in enclosed environments (Collin & Pettigrew, 1989; Collin *et al*., 2000; de Busserolles, 2013). Horizontal streaks represent elongated zones of high cell density, allowing a panoramic perception, more common in open water species (Collin & Pettigrew, 1989; Collin *et al*., 2000; de Busserolles, 2013). Many open water teleosts present both visual specializations, a temporal area centralis probably used during feeding and a horizontal streak to detect intra- or interspecific movements (Collin & Pettigrew, 1989; de Busserolles, 2013).

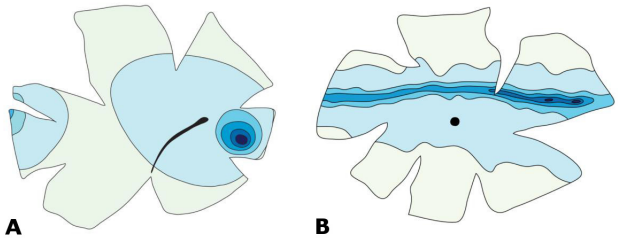

Figure 3 – RGCs topographic maps showing different visual specializations. A) Area centralis on coral cord *Cephalopholis miniatus*; B) horizontal streak on small-spotted dogfish *Scyliorhinus canicula*. From de Busserolles (2013).

RGCs and PRs peak densities allow determining the visual sensitivity and acuity, defining light sensitivity and image quality, respectively. Peak cell densities can be as high as 7.4 x 10^3 cell/mm^2 in RGCs and to 119 x 10^4 cell/mm^2 in PRs (Wagner *et al*., 1998; de Busserolles, 2013).

Visual acuity might be expressed as the spatial resolving power (SRP), calculated from the peaks of RGCs density (Collin & Pettigrew, 1989; Ullmann *et al*, 2011; de Busserolles, 2013). SRP is determined by the number of cells subtended by one degree of visual arc, e.g., the visual angle (Collin & Pettigrew, 1989; Ullmann *et al*., 2011; de Busserolles, 2013). An evolutionary relation between visual acuity and the animal's depth range can be expected, once acuity is limited by the available light (Warrant & Locket, 2004; McFall-Ngai *et al*, 1986; de Busserolles, 2013). In teleosts, visual acuity is also influenced by non-retinal characteristics of the eye, such as the pupil diameter, which constrains the received light (Warrant & Locket, 2004; de Busserolles, 2013; Nillson *et al*., 2004). In fact, acuity is directly related to eye size and lens diameter (Pankhurst, 1987; Collin & Pettigrew, 1989; Douglas *et al*., 1998; de Busserolles, 2013). As stated, visual

sensitivity is more important to deep-sea fish than visual acuity. Sensitivity can be given by the level of PRs-RGCs convergence/summation ratio (Collin & Pettigrew, 1989; Ullmann *et al*, 2011; de Busserolles, 2013). A high degree of PRs-RGCs convergence ratio is linked to high visual sensitivity and it increases with fish growth (7:1 to 300:1) (McNulty, 1976; Locket, 1980).

1.2.Lanternfish vision

Myctophids (or lanternfishes) are mesopelagic fishes belonging to the diverse family Myctophidae that includes about 250 species and 33 genera in two sub-families: Myctophinae and Lampanyctinae (Moser *et al.*, 1984; Catul *et al*., 2011). These fishes are characterized by high abundance populations and worldwide distribution, representing more than 20% of the oceanic ichthyofauna and occupying upper and lower mesopelagic zones (Catul *et al*., 2011; Sutton, 2013). Myctophids' development occurs mainly in the epipelagic zone where they carry most activities such as feeding and reproduction (Catul *et al*., 2011). Myctophids are dioecious pelagic spawners and females are oviparous with low fecundity rate (Catul *et al*., 2011). Eggs and pre-metamorphosis larvae are planktonic, and larvae are daytime feeders, contrary to mesopelagic post-metamorphic individuals and adults (Moser & Ahlstrom, 1972; Catul *et al*., 2011). Adult myctophid's size range from 3 to 35 cm (Hulley, 1994), with lifespans of one year for tropical species and more than five years in temperate zones (Moser & Ahlstrom, 1972).

Lanternfishes are also a major component of the DVM aggregations of mesopelagic species. Lanternfishes feed during the night, from dusk to dawn, following zooplankton DVM (Catul *et al*., 2011; Vieira, 2011). They switch between day inactivity in the mesopelagic zone to night activity in the epipelagic zone where they feed on zooplankton, mainly copepods, euphasiids and amphipods (Shreeve *et al*., 2009). Patterns in diel vertical movements depend on life stage, sex, latitude, hydrography and season, and do not always involve the entire population (Catul *et al*., 2011). Therefore, myctophids have an important role in biogeochemical fluxes, acting as a trophic link between zooplankton and their predators (e.g., marine mammals, seabirds and cephalopods) (Trueman *et al.,* 2014).

Myctophids possess ventrolateral photophores (Fig. 4) used for counterillumination, but also for intraspecific and, perhaps, interspecific communication (Moser & Ahlstrom, 1972; Mensinger & Case, 1997). Probably, for intraspecific communication, myctophids rely on species-specific photophore emitting light patterns to communicate within a swimming school, individual identification and even courtship signalling (Cocker, 1978; Turner *et al*., 2009; Haddock *et al*., 2010). Some species present gender specific luminous caudal glands, either supracaudal (males) or

infracaudal (females) (Salvanes & Kristoffersen, 2001; Catul *et al*., 2011). Some myctophid species possess luminous organs, which are opaque patches of luminous tissue that differs structurally and in light signal from the photophores (Moser & Ahlstrom, 1972; Barnes & Case, 1974; Edwards & Herring, 1977). These organs present a different physiological control and produce quicker and brighter flashes than photophores (Barnes & Case, 1974; Edwards & Herring, 1977). Additionally, some species show luminous patches on the head which produce bright flashes that may confuse predators and illuminate prey (e.g. *Ceratoscopelus* spp. and *Diaphus* spp.) (Barnes & Case, 1974; Edwards & Herring, 1977; Haddock *et al*. 2010). Head photophores or luminous patches enhance the myctophids' visual acuity but may also expose them to predators (Cocker, 1978; Mensinger & Case, 1997; Haddock *et al*., 2010; Catul *et al*., 2011). Some myctophid species might even be able to detect long wavelength light emitted by other deep-sea species (Turner *et al*., 2009; Haddock *et al*., 2010).

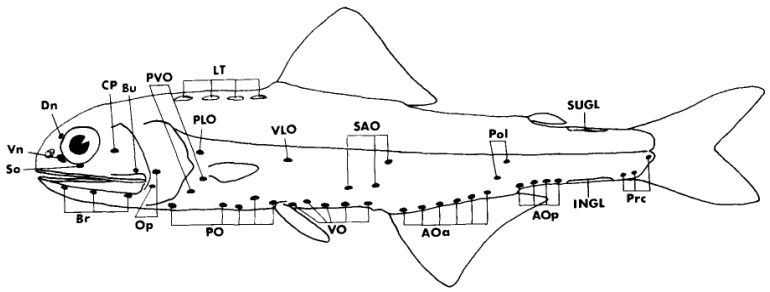

Figure 4 - Scheme of generic myctophid photophore pattern. From Moser *et al.* (1984). Acronyms for photophore groups are presented.

Besides the general vision characteristics shared by deep-sea fishes, most myctophids are mainly adapted to their bioluminescence λImax (469-474 nm), as there is a wide interval of wavelength from their prey or their predators to themselves (Partridge *et al*., 1988; Turner *et al*., 2009). Light modulation is under neural control through physiological processes involving nitric oxide; myctophids are able to control ventral photophores luminescence to almost instantly match the downwelling light (Cocker, 1978; Young *et al*., 1979; Mensinger & Case, 1997; Krönström & Mallefet, 2010). As this wavelength match is not perfect, some predators may distinguish their preys' counter-illumination silhouette (Young *et al*., 1979; Johnsen *et al*., 2004; Turner *et al*., 2009).

The majority of myctophids present retinas with single-pigment rhodopsin, λmax of 480-492 nm (Mensinger & Case, 1997; Hasegawa *et al*., 2008). However, according to Mensinger & Case (1997), Hasegawa *et al*. (2008) and de Busserolles (2013) there are a few double-pigmented with

rhodopsin/pophyropsin or two rhodopsins species, for instance in the genus *Myctophum*. Non-paired rhodopsin/porphyropsin may be an adaptation for detecting stomiid predators' red light (porphyropsine) and shorter-wave light (rhodopsin) (Mensinger & Case, 1997; Hasegawa *et al*., 2008). Hasegawa *et al*. (2008) also suggest the disparity of λmax between the two pigments may indicate not only larger spectral range but also colour vision for these deep-sea fishes. Two additional retinal specializations are present in myctophids: a fundal pigmentation, probably a modified pigment of epithelial cells of a visual specialization important at larval stages; and a photostable yellow pigment, only found in species of the subfamily Myctophinae, which seems to be used to enhance contrast and improve the detection of bioluminescent signals (de Busserolles, 2013).

1.3. Aims and objectives

The main aim of this study is to contribute to the knowledge of how retinal organization can reflect the visual needs of myctophids in the mesopelagic zone.

The specific objectives are:

- to determine visual specializations of photoreceptors and retinal ganglion cells
- to estimate visual acuity and sensitivity, particularly sensitivity to downwelling sunlight and sensitivity to bioluminescence by analysing the topography of photoreceptors, and retinal ganglion cell densities in adult myctophids of different species;
- to interpret the data obtained in relation to morphometric, phylogenetic, environmental and behavioural data available for the myctophid species studied.

2. Materials and methods

2.1.Collection of specimens

Adult myctophids were collected during the R/V Poseidon cruise P446 at Senghor Seamount (Fig. 5), which is located ca. 60 nm east to the Island of Sal, Cape Verde (Central Eastern Atlantic), on February 2013. Six IKMT (Isaac-Kid Mid-Water Trawl) trawls were conducted between the surface and 500 m depth from dusk to midnight. Immediately after recovery of the catch, fishes were measured for total length (± 1 mm) and preserved in a seawater and 4% paraformaldehyde solution, until identification and dissection. All the fishes were captured under the same conditions except *Symbolophorus* sp., which was found on the deck (Table I).

Note: This part of the study was not performed by the author. The collection of specimens was carried out by Rui Pedro Vieira.

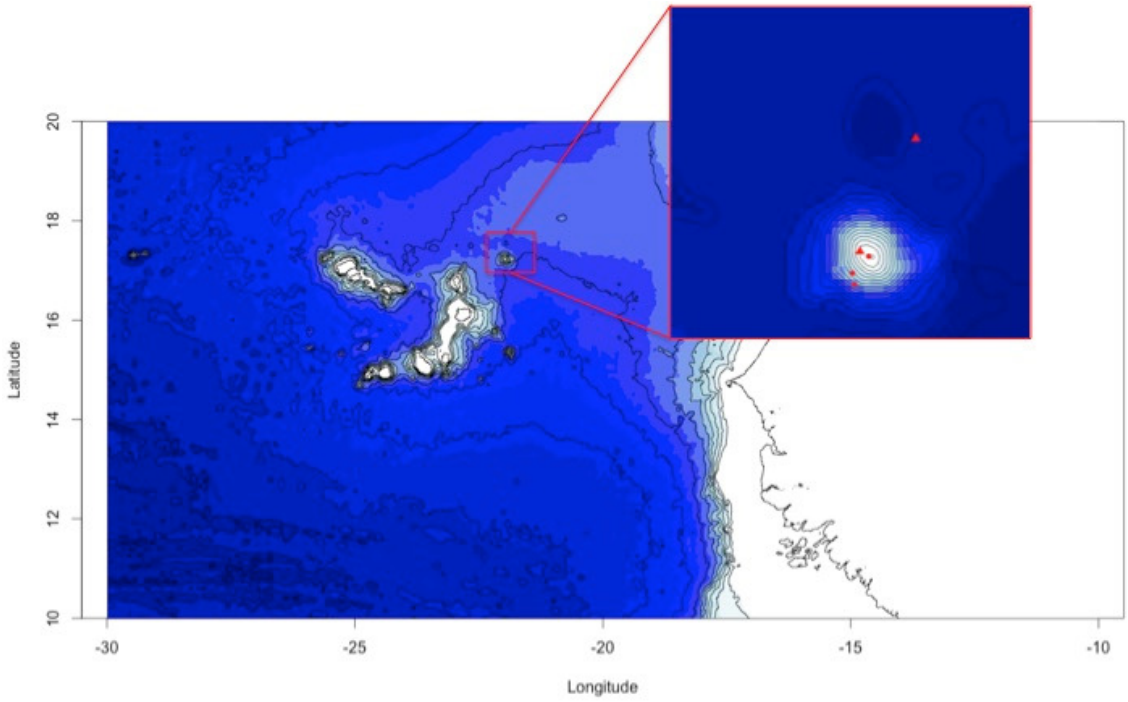

Figure 5 – Bathymetric maps showing the sampling stations of R/V Poseidon cruise P446 at Senghor Seamount, next to Cape Verde archipelago. Sampling stations for specimens of this study are marked with triangles (map produced using marmap package in R: Pante & Simon-Bouhet, 2013).

2.2.Retinal observations

Seven individuals were selected from different species identified according to Hulley (1989): *Diaphus holti*, *Diaphus rafinesquii*, *Symbolophorus* sp., *Lampadena* sp., *Hygophum taaningi*, *Lepidophanes guentheri*, and *Ceratoscopelus warmingii* (Table 1).

Table I – Summary of the material used in this study and respective sampling stations. UTC=Universal Time Coordinated; Lat=latitude; Lon=longitude.

Species	N	Station	Date	Time	Position		Depth	Gear
				(UTC)	Lat	Lon	m	
Diaphus rafinesquii	1	POS446/508-1	10.02.2013	19:59	17° 31.84' N	21º 50.96' W	<500	IKMT
Diaphus holti	1	POS446/513-1	11.02.2013	19:57	17° 14.34' N	21° 59.64' W	<500	IKMT
Lampadena sp.	1	POS446/513-1	11.02.2013	19:57	17° 14.34' N	21° 59.64' W	<500	IKMT
Hygophum taaningi	1	POS446/513-1	11.02.2013	19:57	17° 14.34' N	21° 59.64' W	<500	IKMT
Lepidophanes guentheri	1	POS446/513-1	11.02.2013	19:57	17° 14.34' N	21° 59.64' W	<500	IKMT
Ceratoscopelus warmingii	1	POS446/513-1	11.02.2013	19:57	17° 14.34' N	21° 59.64' W	<500	IKMT
Symbolophorus sp.	1	n/a	08.02.3013	n/a	17º 11.141' N	21º 57.263' W	n/a	n/a

For each individual, full body photographs were taken with a digital camera, while eyes were photographed under a dissection microscope. The following morphometric parameters were measured using ImageJ 1.47V (Rasband, 1997-2014): 1. Total and Standard Lengths[1] (TL and SL, respectively); 2. Rostrocaudal and Dorsoventral Eye Diameters (RC-ED and DV-ED, respectively); 3. Lens Diameter (LD).

Fishes eyes were enucleated and the retinas extracted and observed under light microscopy (100x objective for PRs and 40x for ACs/RGCs) for retinal wholemount analyses of PRs, ACs and RGCs (Appendix I). This procedure allows one to develop density topographic maps for these neural cells, and subsequently to identify visual specializations and density peaks of neural cells (Collin & Pettigrew, 1989; Ullmann *et al*., 2011; de Busserolles, 2013). Horizontal scans of the retinas were performed to define sampling areas (SAs). Coordinates were registered for each SA and neural cells were counted to estimate cell densities. SAs coordinates allowed to create topographic maps that incorporate cell density values from 200 selected SAs. Finally, a colour gradient was used to match the cell density value in order to represent the distribution of cell

[1] Total length is measured to the tip of the tail while standard length is to the base of the tail (Hulley, 1989).

densities along the retina. Retinas were stained with Cresyl violet to distinguish RGCs and ACs. Cell counts and production of retinal maps were done with ImageJ 1.47V and GIMP 2.8.10. The Schaffer Coefficient of Error (CE) was applied to ensure cell number estimation:

$$CE=1/\sqrt{Q}$$, where Q represents the number of cells counted.

2.3. Visual parameters estimations

Visual parameters were estimated following Collin & Pettigrew (1989), Ullmann *et al*. (2011) and de Busserolles (2013). Visual sensitivity was calculated from PRs-RGCs convergence, from the peak densities of neural cells. Visual acuity, expressed as SRP, was calculated from the peaks of RGCs density. For SRP estimates, Matthiessen's ratio was used to calculate the distance from the centre of a lens to the retina (posterior nodal distance, PND). Mattthiessen's ratio states that the focal length in fishes is ≈2,55 the radius of the lens:

$$PND = 2{,}55 \times r$$, where r is the radius of the lens.

The angle (α) subtending 1 mm on the retina is given by:

$$\tan(\alpha) = 1\text{mm}/PND.$$

SRP is determined by the number of cells.mm^{-1} subtended by 1 degree of visual arch:

$$\text{Cells per degree} = \text{density at peak area}/PND.$$

To distinguish the light-dark boundaries for 1 cycle of grating of the highest resolvable frequency, at least 2 cells are needed:

$$\text{SRP (cycles per degree)} = \text{cells per degree}/2.$$

Visual sensitivities to downwelling light and bioluminescent point sources were estimated for the different specimens.. Sensitivity to downwelling light (S, extended light scene, expressed in mm^{-2}.sr^{-2}) was calculated by the following equation:

$$S = \left(\frac{\pi}{4}\right)^2 \left(\frac{1}{1.275}\right)^2 d^2 \left(1 - e^{-kl}\right).$$

[2] Steradian – SI Unit for solid angle (Warrant & Locket, 2004).

where *d*, *k* and *l* are the diameter, absorption coefficient and outer segment length of the PRs, respectively. As *k* is fixed at 0.035 μm^{-1}, which is the average value for vertebrates, and 1,275 represents a constant that relates the size of pupil and lens, in this equation, *S* is related to PRs diameter and outer segments length (de Busserolles, 2013). The diameter, *d,* was measured in median density areas of PRs in the retina. The length *l* was obtained from de Busserolles (2013).

Sensitivity to bioluminescent flashes (*N*, point source of light, in photons) is given by the following formula:

$$N = \frac{EA^2}{16r^2} e^{-\alpha r}(1 - e^{-kl}).$$

where *E* represents the number of photon emitted at the source, *A* is for the pupil diameter (meters), *r* is the distance (meters) between the light source and the eye, α represents the attenuation coefficient of bioluminescence (combining the scattering and absorption of light by the water molecules), and *k*, *l* are the absorption coefficient and outer segment length of the PRs, respectively. As the pupil diameter was replaced by the lens diameter for *A*, as *E* was set at 10^{10} photons, *r* at 1m, α at 0,05 m^{-1}, and k at 0.035 μm^{-1}, *N* is related to the lens' size and the outer segment length of PRs (see Warrant & Locket, 2004; and de Busserolles, 2013).

3. Results

3.1.Distribution of neural cells density

The analysed retinas were degraded and, consequently, mapping of the PRs and RGCs/ACs from the same eye was only possible for *H. taaningii* and *C. warmingii* specimens. Yellow pigmented patches were not observed, and fundal pigmentation was not distinguishable in most of the retinas analysed. No retinal tapeta were observed.

3.1.1. Photoreceptors

All the analysed myctophid species present pure-rod retinas with a single rod type, and cells densely packed with a hexagonal arrangement. Rod densities[1] varied within each individual retina and between individuals (in this case corresponding to different species) (Fig. 6). Peaks of PRs densities are shown in Table II. Rod densities are higher for *Diaphus rafinesquii*, *Symbolophorus* sp. and *Lampadena* sp. and lower for *Hygophum taaningi* and *Lepidophanes guentheri*.

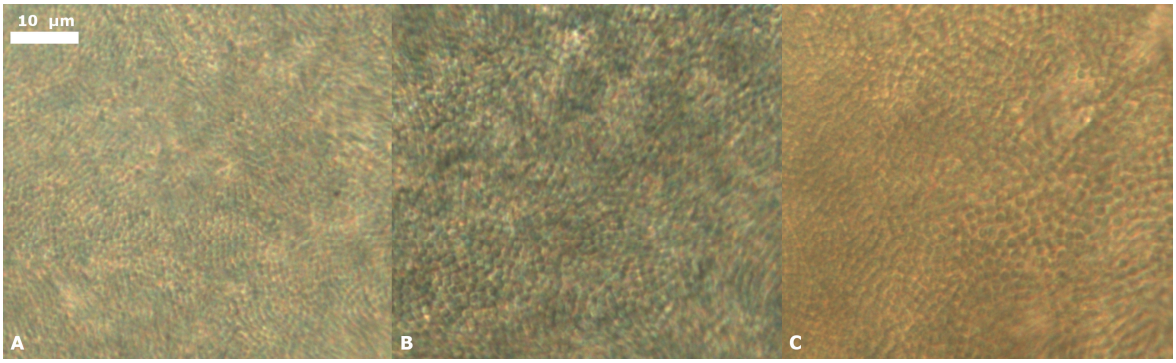

Figure 6 – Photographs of rods under a 100x objective of a light microscope, showing PRs density variation along the same retina (A, B) and between species (A,C). A) Peak density of *Ceratoscopelus warmingii* (1060 x 10^3 cells.mm^{-2}); B) low density zone of *C. warmingii* (550 x 10^3 cells.mm^{-2}); C) peak density of *Hygophum taaningi* (660 x 10^3 cells.mm^{-2}). The scale is the same for all photographs.

[1]As cell density is inversely proportional to cells diameter in a fixed area (100µm^2), this last parameter was not included.

Table II – Rods density (x 10^3 cells.mm^{-2}) for analysed species. Schaeffer Coefficient of Error (CE) refers to the average values. Average was calculated from 200 SAs counting. Total cells' values were estimated from cells' average density and respective area (see Appendix I for details).

Species	PRs				
	Minimum	Peak	Total	Average	CE
Diaphus holti	448	1096	28380973	767	0.04
Diaphus rafinesquii	644	1250	34526933	863	0.03
Symbolophorus sp.	586	1318	66045086	821	0.03
Lampadena sp.	624	1368	64007333	955	0.03
Hygophum taaningi	212	692	17788400	445	0.05
Lepidophanes guentheri	340	752	8855013	466	0.05
Ceratoscopelus warmingii	420	1090	37699189	768	0.04

As identified by several authors (e.g. Collin & Pettigrew, 1989, Collin *et al*., 2000, and de Busserolles, 2014), specific patterns of rods suggest visual specializations. *Diaphus holti* present an arch through the dorsal-temporal part of the retina with peak density in the ventral-temporal zone (Fig. 7A) with 1096 x 10^3 cells.mm^{-2}. *Lampadena* sp. also shows a dorsal-temporal arch, with a peak density of 1368 x 10^3 cells.mm^{-2} located in the dorsal part of the retina (Fig. 7D). For *D. rafinesquii*, the arch is located across the nasal-ventral-temporal region of the retina, with the peaks of rods' density in the retina's temporal and nasal zones (Fig. 7B) with 1250 x 10^3 cells.mm^{-2}. *Symbolophorus* sp. and *H. taaningi* present streak-like specializations. *Symbolophorus* sp. shows a ventral streak with peak density, located in the ventral zone of the retina (Fig. 7C) of 1318 x 10^3 cells.mm^{-2}. However, the streak specialization for *H. taaningi* is located through the nasal-ventral zone of the retina (Fig. 7E) showing a peak density of 692 x 10^3 cells.mm^{-2}. Contrary to the former species, *L. guentheri* and *C. warmingii* present ring specializations, showing higher cell densities between the centre and the periphery of the retina in a ring-like shape. The first species shows a peak cell density of 752 x 10^3 cells.mm^{-2} across the retina (Fig. 7F) while *C. warmingii* present temporal-ventral peak cell density (Fig. 7G) with 1090 x 10^3 cells.mm^{-2}.

Except for *Symbolophorus* sp. and *H. taaningi*, the aphakic gap projection appears to match the rods' peak density areas (Fig. 7).

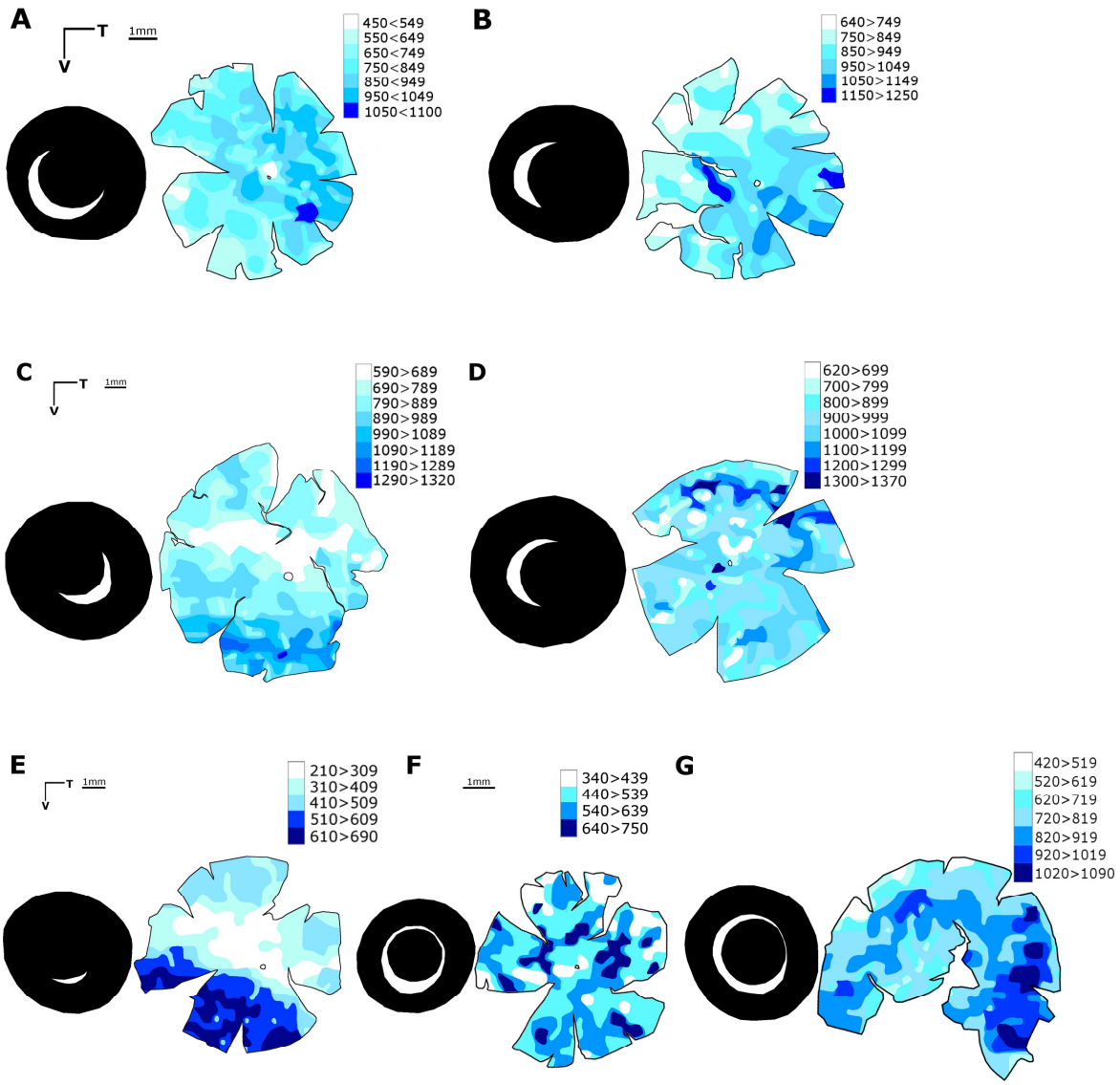

Figure 7 - Topographic maps of rods density (x 10^3 cells.mm^{-2}) for the analysed species, with respective aphakic gap on the left. A) *Diaphus holti*, B) *D. rafinesquii*, C) *Symbolphorus* sp., D) *Lampadena* sp., E) *Hygophum taaningi*, F) *Lepidophanes guentheri*, and G) *Ceratoscopelus warmingii*. T= Temporal, V= Ventral. Scale bar is the same for the maps side by side, except for F. Aphakic gaps are represented by the white band.

3.1.2. Amacrine cells and retinal ganglion cells

All the analysed species showed a similar arrangement and densities of ACs and RGCs. The analysed retinas suggests that ACs present greater densities and higher variance (Table III), "surrounding" RGCs (Fig. 8). Contrary to PRs, CE is higher than 0,1 for RGCs and ACs, probably representing an inaccurate counting. This pattern was predictable, once RGCs and ACs were observed and counted under a 40x objective with less than 200 SAs.

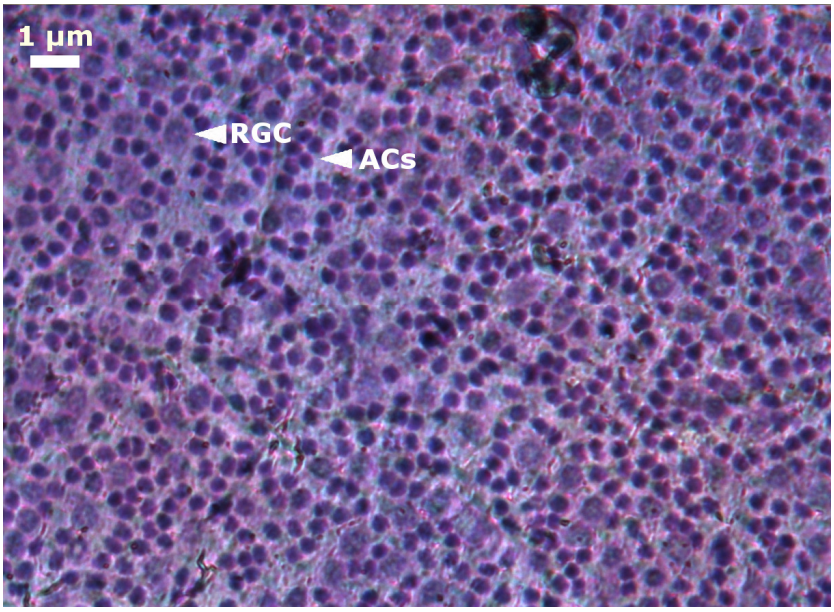

Figure 8 –Photograph under 40x objective of light microscope, showing RGCs and ACs arrangement for *Ceratoscopelus warmingii*.

Table III – ACs and RGCs densities (x 10^3 cells.mm^{-2}). Schaeffer Coefficient of Error (CE) refers to the average values. Total cells' values were estimated from cells' average density and respective area.

Species	Neural cell type	Neural cells density				
		Minimum	Peak	Total	Average	CE
Diaphus holti	ACs	43	103	2548394	69	0.12
	RGCs	10	33	582490	16	0.25
Diaphus rafinesquii	ACs	33	110	2473958	62	0.13
	RGCs	10	27	621875	16	0.25
Symbolophorus sp.	ACs	16	56	2537250	32	0.18
	RGCs	10	18	1032804	13	0.28
Lampadena sp.	ACs	16	44	1896770	28	0.19
	RGCs	10	20	951400	14	0.27
Hygophum taaningi	ACs	16	44	1237007	31	0.18
	RGCs	10	22	558912	14	0.27
Lepidophanes guentheri	ACs	22	50	620792	33	0.17
	RGCs	10	18	267129	14	0.27
Ceratoscopelus warmingii	ACs	10	50	1245529	25	0.20
	RGCs	8	20	613590	12	0.28

In all cases ACs and RGCs density patterns were similar for the same specimen and densities of these cells were always higher in the periphery of the retinas (Fig. 9).

Except for *Symbolophorus* sp. and *L. guentheri,* which do not display clear specializations (Fig. 9C2 and 9F2, respectively), the analysed species present areae specializations for RGCs. *Diaphus holti* presented an area temporalis (Fig. 9A2) with a density peak of 33 x 10^3 cells.mm^{-2}. *Diaphus rafinesquii* shown an area ventro-temporalis (Fig. 9B2) with a density peak of 27 x 10^3 cells.mm^{-2}. *Lampadena* sp. presented an area dorso-temporalis (Fig. 9D2) with 20 x 10^3 cells.mm^{-2}. *Hygophum. taaningi* seems to have an area temporalis and an area rostralis (Fig. 9E2) with density peaks of 18 x 10^3 cells.mm^{-2}. The latter indication must be considered with caution, because the temporal zone of the retina was accidentally damaged during the tissue preparation. *C. warmingii* presented an area ventro-rostralis (Fig. 9G2) with a density peak of 20 x 10^3 cells.mm^{-2}.

Aphakic gap projections appears to be coincident with higher densities of RGCs, except for *Symbolophorus* sp. and *H. taaningi* (Fig. 9).

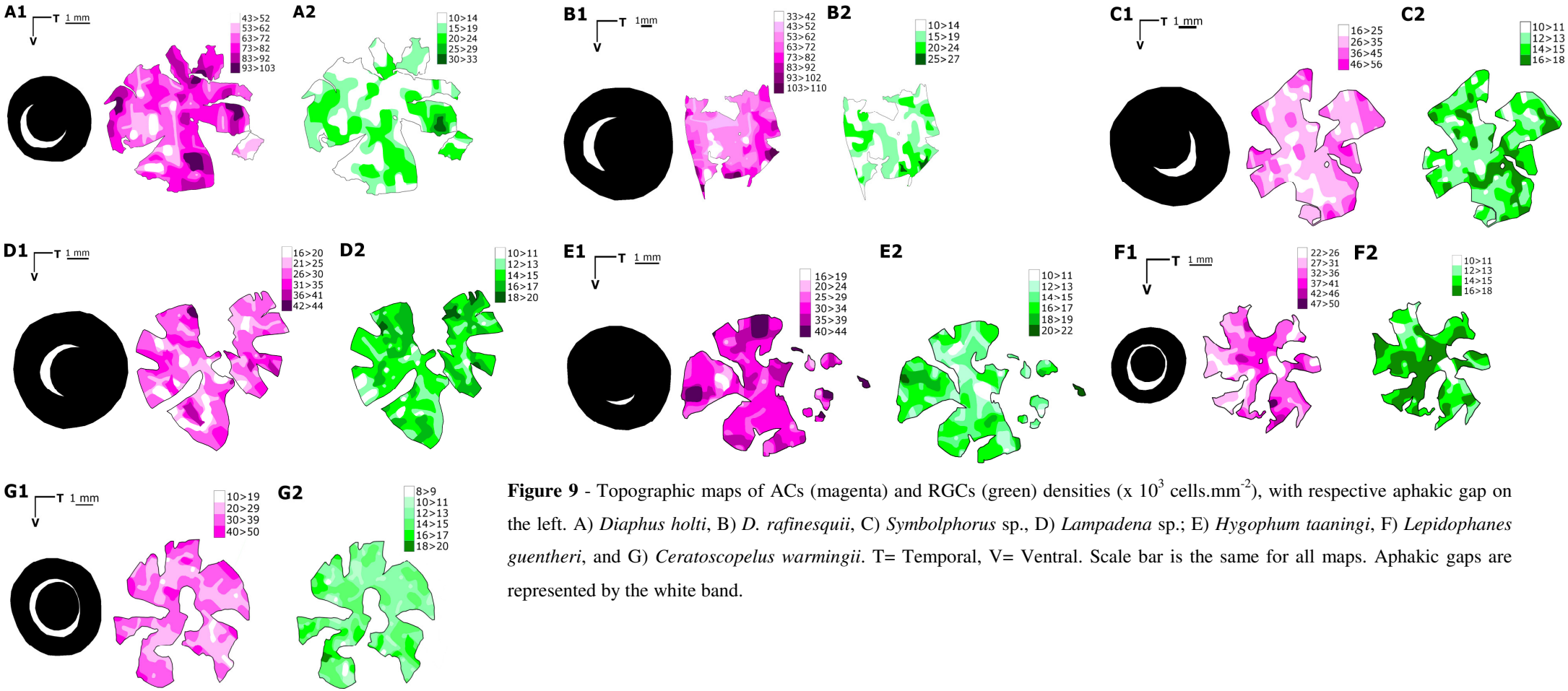

Figure 9 - Topographic maps of ACs (magenta) and RGCs (green) densities (x 10^3 cells.mm^{-2}), with respective aphakic gap on the left. A) *Diaphus holti*, B) *D. rafinesquii*, C) *Symbolphorus* sp., D) *Lampadena* sp.; E) *Hygophum taaningi*, F) *Lepidophanes guentheri*, and G) *Ceratoscopelus warmingii*. T= Temporal, V= Ventral. Scale bar is the same for all maps. Aphakic gaps are represented by the white band.

3.2. Visual acuity and sensitivity

Estimations of visual acuity and sensitivity, given by PRs-RGCs convergence and SRP, respectively, are presented in Table IV. Acuity and sensitivity seems to not vary greatly between species, but both parameters were higher for *Symbolophorus* sp. and *Lampadena* sp. Acuity was lower for *L. guentheri* while *D. holti* and *H. taaningi* showed lower sensitivity values.

Sensitivity to downwelling light (*S*) and bioluminescence (*N*) seems to not vary much between species (Table IV). As *l* value for *Diaphus rafinesquii* and *Lepidophanes guentheri* was not found in the literature available, data on sensitivity to downwelling light and bioluminescence for this species is not presented. *Diaphus holti* showed the lowest values for sensitivity to sunlight and bioluminescence, while *Symbolophorus* sp. and *Lampadena* sp. presented higher sensitivity to bioluminescence and lower sensitivity to downwelling light. *Hygophym taaningi* and *C. warmingii* presented low sensitivity to bioluminescence, but high sensitivity to sunlight.

Table IV – Spatial resolving power (SRP, in cycles per degree), PRs-RGCs convergence ratio, lens diameter (LD), diameter (*d*, µm) and outer segment length (*l*, µm) of photoreceptors, and visual sensitivity to downwelling light (*S*, μm^2.sr) and to bioluminescence (*N*, in photons).*l value* from de Busserolles (2013).

Species	SRP	PRs-RGCs convergence	LD	*d*	*l*	Visual sensitivity	
						S	*N*
Diaphus holti	4.88	33:1	2.3	0.7	45.0	0.16	2559
Diaphus rafinesquii	4.70	46:1	2.5	0.8			
Symbolophorus sp.	5.06	73:1	3.3	0.9	41.1	0.21	5028
Lampadena sp.	5.13	68:1	3.2	0.8	42.5	0.20	4712
Hygophum taaningi	4.34	31:1	2.6	1.0	44.7	0.32	3057
Lepidophanes guentheri	2.58	42:1	1.6	0.9			
C.eratoscopelus warmingii	4.23	55:1	2.6	1.0	49.2	0.31	3326

3.3. Morphologic parameters

The morphometric parameters of the eyes are given in Table V. Higher values were found for the larger specimens analysed *Symbolophorus* sp. (SL = 7,19 cm) and *Lampadena* sp. (SL = 7,50 cm). *Lepidophanes guentheri* presented smaller eyes in relation to the size of the fish. Luminous patches are present only for *Diaphus* species and *C. warmingii*, but other external characters indicating sexual dimorphism were only detected in *D. holti*, *D. rafinesquii*, *Symbolophorus* sp. and *H. taaningi*.

Table V - Morphometric traits analysed in this study. SL=Standard length, RC-ED=rostrocaudal eye diameter, DV-ED=dorsoventral eye diameter, LD=lens diameter.

Species	SL (cm)	Eyes morphometrics (mm)			Luminous patches	Sexual dimorphism
		RC-ED	DV-ED	LD		
Diaphus holti	4.67	5.46	5.55	2.33	Yes	Yes
Diaphus rafinesquii	5.27	5.49	5.47	2.49	Yes	Yes
Symbolophorus sp.	7.19	7.78	7.99	3.33	No	Yes
Lampadena sp.	7.50	7.76	7.53	3.20	No	No
Hygophum taaningi	5.06	5.77	5.63	2.55	No	Yes
Lepidophanes guentheri	5.42	3.58	3.61	1.61	No	No
Ceratoscopelus warmingii	6.41	6.27	6.16	2.61	Yes	No

4. Discussion

4.1.Topography of neural cells' density and visual parameters

4.1.1. Photoreceptors

All the species analysed present pure-rod retina with high density of PRs, reflecting the known high visual sensitivity of myctophids' retinas (O'Day & Fernandez, 1976; Pankhurst, 1987; Wagner *et al*., 1998; Sabatés *et al*., 2003; de Busserolles, 2013). High visual sensitivity of myctophids shows an adaptation to the dim and monochromatic light regimes characteristic of the mesopelagic zone (Douglas *et al*., 1995; Douglas *et al*., 1998; Turner *et al*., 2009). Additionally, these fishes use bioluminescence for communication, feeding and reproduction (Cocker, 1978; Mensinger & Case, 1997; Turner *et al*., 2009; Haddock *et al*., 2010). Therefore, the perception of a faint point of light is essential to their ecological success.

Distribution patterns of rod densities reflect visual specializations, which can be associated to the visual needs and behaviour of the fish (Collin & Pettigrew, 1989; Collin *et al*., 2000; de Busserolles, 2013). The analysed myctophid species present different rod specializations. Rod densities, given in Table II, differed within the same retina but also between species, suggesting species-specific visual needs (see Fig. 7). In the analysed species the position of the aphakic gap allows the projection of the light on the retinal zones with high PRs density, except in the species presenting streak-like PRs specialization. The aphakic gap allows "extra" light on the retina (Warrant & Locket, 2004; de Busserolles, 2013), while photoreceptors function is to maximize the photon catch (Yokoyama & Yokoyama, 1996; Warrant & Locket, 2004; Turner *et al*., 2009). Consequently, the retinal zones with higher photon incidence are also the more sensitive areas of the retina, enhancing eye's photon catch. This concordance may depend upon the type of PRs specialization, but the examination of a larger number of individuals is required to confirm the exception found in the species with a streak-like specialization of (e.g. *Symbolophorus* sp. and *Hygophum taaningi*,) also observed by de Busserolles (2013) in other myctophids. *Diaphus holti* and *Lampadena* sp. showed a dorsal-temporal arch, meaning that the incident light in this region has origin in the lower frontal area of the fish visual field. This type of arch specializations may be used to detect bioluminescence sources from below (de Busserolles, 2013). *Diaphus rafinesquii* shows a nasal-ventral-temporal arch, capturing light from the upper frontal part of the fish's visual field. This arrangement may be linked to enable the ability to distinguish predators or prey silhouettes against the background (de Busserolles, 2013). The distinction of upper silhouettes may also be assigned to the ventral streak-like specialized retinas in *Symbolophorus* sp. and *H. taaningi*. Ring specializations observed in *Lepidophanes guentheri* and *Ceratoscopelus warmingii* might be related to the light projected by the circumlental aphakic gap (see Fig 7). The peak density of rods

in the temporal-ventral zone of *C. warmingii* retina suggests this region has an important role receiving the light coming from the upper front of the fish.

The circumlental aphakic gap allows an increased visual field in every direction. PRs ring specializations are present in visual generalists or fishes that do not rely much in vision as an important sensorial system (de Busserolles, 2014). Most likely, *L. guentheri* and *C. warmingii* are visual generalists, once they have several visual stimuli from different directions. Myctophids are able to produce bioluminescent light, but are also subjected to great light gradients. Therefore, they seem to rely strongly on vision to succeed in such environment (Young *et al*., 1979; Partridge *et al*., 1988; Johnsen *et al*., 2004; Turner *et al*., 2009), namely by using it to avoid predators and forage preys (Catul *et al*., 2011: Murphy *et al*., 2007; Shreeve *et al*., 2009).

4.1.2. Amacrine cells and retinal ganglion cells

Myctophid neural cells densities here estimated are higher than those obtained by de Busserolles (2013). This might be explained as an observations bias, but also due to the degradation of the retinas and some handling procedures (see Appendix II).

ACs and RGCs densities do not seem to vary much across the retina or between species (see Table III). According to several authors (Collin & Pettigrew, 1989; Wagner *et al*., 1998; Warrant & Locket, 2004) this is an indication of low visual acuity. Considering that mesopelagic depths are characterized by dim and monochromatic light, acuity is not crucial to the animals that inhabit this oceanic zone (Pankhurst, 1987; Warrant & Locket, 2004; de Busserolles, 2013). Under these light regimes the detection of a faint light signal (sensitivity) may be far more important for mesopelagic fishes than perceiving images with great definition (acuity).

ACs and RGCs density estimates were always higher in the retinal periphery and the topography of these two types of neurons revealed some similarities (see Fig. 9). Both types of neural cells show similar distributions (Collin & Pettigrew, 1989). However, ACs functions are still not well understood, and the inclusion of these neural cells in SRP calculations may led to an overestimation of acuity (Wagner *et al*., 1998; de Busserolles, 2013). Additionally, since RGCs represent the gateway of visual information to the brain (Wagner *et al*., 1998; Warrant & Locket, 2004), only this cell type will be discussed below.

Even if RGCs densities showed little variation across the retina in the analysed species, area specializations are present, and this indicates that visual acuity is important for these fishes' visual capabilities (Collin & Pettigrew, 1989; Wagner *et al*., 1998; Collin *et al*., 2000; de Busserolles, 2013). Although less precisely than for PRs, aphakic gaps are also coincident with the RGCs peak density zones. The exceptions are the PRs streak specialized retinas of *Symbolophorus* sp. and *H. taaningi*. These two species also differ in their relative (spatial) alignment of the PRs and RGCs

density peaks. As the light emitted by counterillumination presents a wavelength range similar to the downwelling light (Partridge *et al*., 1989; Turner *et al*., 2009; Haddock *et al*., 2010) and myctophids communicate with light patterns (Moser & Ahlstrom, 1972; Moser *et al*., 1984; Mensinger & Case, 1997; Catul *et al*., 2011), some acuity is needed to distinct the silhouette of a conspecific from a predator or a prey (Cocker, 1978; Yokoyama & Yokoyama, 1996; Johnsen *et al*., 2004; Turner *et al*., 2009). This PRs and RGCs alignment may allow a better silhouette distinction against the downwelling background light (de Busserolles, 2013), as stated before for the ventral arch specialization of PRs in *D. rafinesquii*. The correspondence of PRs and RGCs peak densities with the aphakic gaps corroborates that visual acuity may also be important for these fishes.

The analysed species presented areae (see Fig. 9), which may reflect similar visual needs for acuity. Exceptions are *Symbolophorus* sp. and *L. guentheri* which do not present any clear RGCs specialization which might be linked to an improved visual sensitivity (de Busserolles, 2013). However, these conclusions should be taken carefully, because RGCs specializations were previously observed in *Symbolophorus* species (de Busserolles, 2013). Differences in the present study and results obtained by de Busserolles (2013) might be explained by the degradation of retinas or methodological issues here. *Diaphus holti*, *D. rafinesquii, Lampadena* sp. and *H. taaningi* present areae temporales reflecting an enhanced acuity in relation to the front visual field of the animal. This may probably facilitate the binocular vision for predation or adaptation to a structurally complex habitat (de Busserolles, 2013), which are ecological traits of myctophids, as previously stated. *Hygophum taaningi* seems to show also an area in the nasal part of the retina that, similar to *C. warmingii* area in the ventral-nasal zone of the retinas but no similar observation was found in the available literature. Eye misorientation might have occurred during the RGCs analysis of *C.warmingii* retina, since de Busserolles (2013) observed an area ventro-temporalis for the same species. Nevertheless, the presence of a ventral areae in the retina of *C. warmingii*, suggests enhanced acuity in relation to the upper part of the visual field, used for distinction of silhouettes above the fish. The case of *H. taaningi* will be addressed later.

4.1.3. Visual acuity and sensitivity

Investigation of the retinas of the seven myctophid species in this study revealed that visual sensitivity was higher for *Symbolophorus* sp. and *Lampadena* sp (see Table IV). Both species presented higher rod peak density and PRs-RGCs convergence, when compared to the other myctophids. *Diaphus holti* and *H. taaningi* presented lower values of visual sensitivity. *Hygophum taaningi* also showed lower rod peaks density, but that was not found in *D. holti*. Visual acuity is calculated using the lens size. This seems to influence and explain the acuity values, as these are higher for *Symbolophorus* sp. and *Lampadena* sp which present the larger lenses (Table V), and

lower for *L. guentheri* with the smaller lens. As referred above, *Symbolophorus* sp. and *L. guentheri* do not present any clear RGCs specialization, which may be linked to increased visual sensitivity. In fact, this may be corroborated by the fact that both species present higher visual sensitivity than acuity, when compared to the other analysed species (Fig. 10).

Sensitivity to downwelling light (*S*) is linked to higher diameter of PRs, while sensitivity to bioluminescent light (*N*) to bigger eyes (see Materials and Methods). PRs diameter are higher for *C. warmingii* (d = 1,00 µm) and *H. taaningi* (d = 1,04 µm) and lower for *D. holti* and *D. rafinesquii* (d = 0,73 and 0,76 µm, respectively), corresponding to the higher *S* values for *C. warmingii* and *H. taaningi* and lower for *Diaphus holti*. As *N* is linked to the size of the eye and the lens, the values for *N* have the same explanation as referred above for visual acuity. Apart from *Diaphus holti* which present the lower values for *S* and *N* (Fig. 11), the analysed species seem to be more sensitive to downwelling light (*H. taaningi* and *C. warmingii*) or to bioluminescent flashes (*Symbolophorus* sp. and *Lampadena* sp.). These results corroborates the early suggestions that *Lampadena* sp. PRs arch specialization may be used to perceive bioluminescent flashes and the ring of *C. warmingii* for perception of silhouettes against the downwelling light background. Low values of visual sensitivity (including *S* and *N*) and high visual acuity estimated for *Diaphus holti* suggests it may rely less on sensitivity to light.

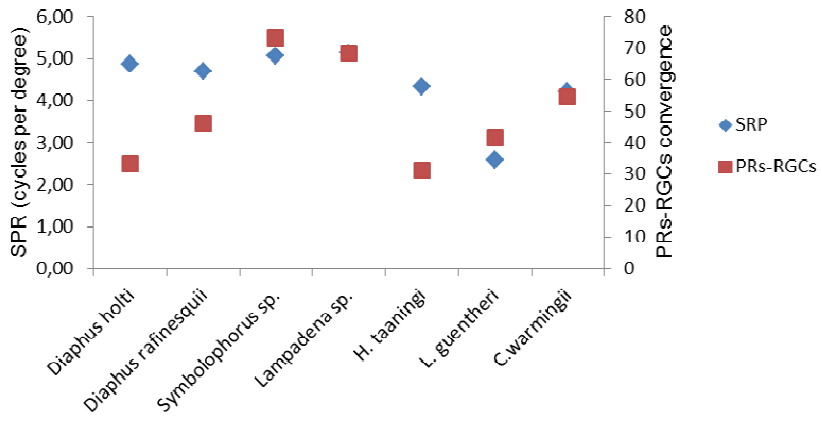

Figure 10 – Dot plot showing the values of visual acuity (SRP, in cycles per degree) and sensitivity (PRs-RGCs convergence).

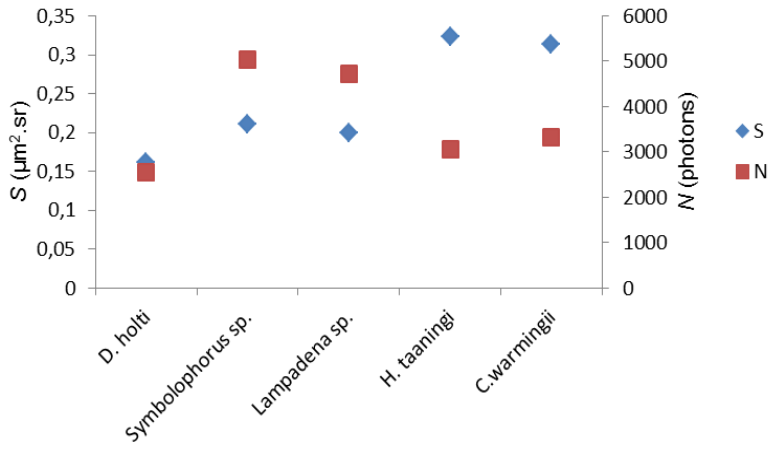

Figure 11 – Dot plot showing the values of sensitivity to downwelling light (*S*, in μm^2.sr) and to bioluminescence (*N*, in photons).

As stated before, aphakic gaps do not coincide with RGCs or PRs peak densities for the PRs streak specialized retinas of *Symbolophorus* sp. and *H. taaningi*. Also RGCs peak densities do not correspond to PRs ones for these two species. *Symbolophorus* sp. is more sensitive to bioluminescence but no clear RGCs specialization (see Fig. 9), so the acuity does not seem important. This corroborates the early suggestion that *Symbolophorus* sp. uses the ventral aphakic gap to detect bioluminescent signals from below. On the other hand, *H. taaningi* is more sensitive to downwelling light and present RGCs specialization, so the acuity seems to have more importance for this species, essentially at the front horizontal axis. *Hygophum taaningi* seems to be better adapted to distinct silhouettes against the downwelling light background on the upper frontal visual field. However, because of the low number of samples this interpretation must be taken with caution.

These results show that visual acuity is relatively low (SRP from 2.58 to 5.13) and sensitivity is high (PRs-RGCs convergence from 31:1 to 73:1) when compared to other deep-sea fish families (e.g. *Argyropelecus sladeni*, SRP = 12:1 and convergence = 8.4; *Alepocephalus bairdii,* SRP = 22.9; *Scopelarchus michaelsarsi*, convergence = 29:1, from Wagner *et al.,* 1998). One could expect that these observations are due to patterns in mesopelagic light regimes, as already explained above. Estimated visual sensitivity is low when compared to other myctophids of the same genera in de Busserolles (2013), but acuity showed higher values. Additionally, estimates of sensitivity to downwelling light are lower, while estimates of sensitivity to bioluminescent light are higher, when compared with the values obtained by de Busserolles (2013). These values divergences may be related with observation bias and methodological issues (see Appendix II).

4.2. Vision and natural history traits in myctophids

4.2.1. Morphology

Eye size is linked to visual parameters, as explained above for SRP and *N*. Species with larger eyes (*Symbolophorus* sp. and *Lampadena* sp.) present higher visual sensitivity (see Table V), probably because the area of retinal tissue is larger and thus contains more rods. Luminous patches and sexual dimorphism do not seem to relate with any retinal characteristics analysed in this study, but a larger sample size is needed to explain these results. de Busserolles (2013) states that myctophids with no luminous patches and with deeper distribution profiles possess higher sensitivity to downwelling light and species with sexual dimorphism possess higher sensitivity (higher rod densities).

4.2.2. Depth range and diel vertical migration

Information on depth ranges was retrieved from Hulley (1989) and vertical migration data is given by Watanabe *et al* (1999). Since it was not possible to identify the specimens of *Symbolophorus* and *Lampadena* to species level, their depth distribution was inferred from the available data on the species of the respective genera present in Cape Verde waters, e.g. *Symbolophorus veranyi* and *Lampadena urophaos*. In fact, species depth ranges do not vary greatly within *Symbolophorus* and *Lampadena* genera (Hulley, 1989). The available information on depth distribution was used to infer, DVM patterns for species that were not analysed in Watanabe *et al.*, (1999). Because all the analysed specimens were adults, only the data on adults was used.

Visual parameters – sensitivity and acuity - appear to be not related with DVM patterns or distances covered by these species, but this was not the case for the PRs specializations. Species with arch specializations are Non-migrators (*D. rafinesquii*) and mid-water migrators (*D. holti* and *Lampadena* sp.). The fact that *D. rafinesquii* inhabits only the upper mesopelagic zone, where downwelling light is the main source of light (Wagner *et al*., 1998; Warrant & Locket, 2004; Yakir *et al*., 2013), is in agreement with the occurrence of a ventral arch specialization to capture light from above and favouring silhouette distinction. Results also suggest that *Diaphus* species might rely less on sensitivity, which can be related with an upper mesopelagic habitat, where downwelling is the main light source (Wagner *et al*., 1998; Warrant & Locket, 2004; Yakir *et al*., 2013). The low DVM distances of *D. holti* and *Lampadena* sp. may explain the retinal specialization found in these species. Arches focus a specific part of the visual field (de Busserolles, 2013), and their specializations in the dorsal region of retinas can detect bioluminescent light from

below. *Lampadena* sp. presents higher sensitivity to bioluminescent flashes than *D. holti* which may be linked to the fact that *Lampadena* sp. inhabits both upper and lower mesopelagic (Fig. 12).

Streak-like specializations were found in surface-migrators (*Symbolophorus* sp. and *H. taaningi*). Their rod specializations capture light from above allowing these species to distinguish silhouettes against the downwelling light (Wagner *et al*., 1998; Warrant & Locket, 2004; Yakir *et al*., 2013). However, *Symbolophorus* sp. seems to be more sensitive to bioluminescent flashes than *H. taaningi*.

Mid-water migrators *L. guentheri* and *C. warmingii* (Fig. 12) showed ring specializations, which were found in visual generalist species (de Busserolles, 2013). This is probably related to the fact that these species are able to perform long vertical migrations and, consequently, are exposed to more dynamic light scenarios. The temporal-ventral peak density of rods in *C. warmingii*'s ring maybe used to further recognise silhouettes from above the fish.

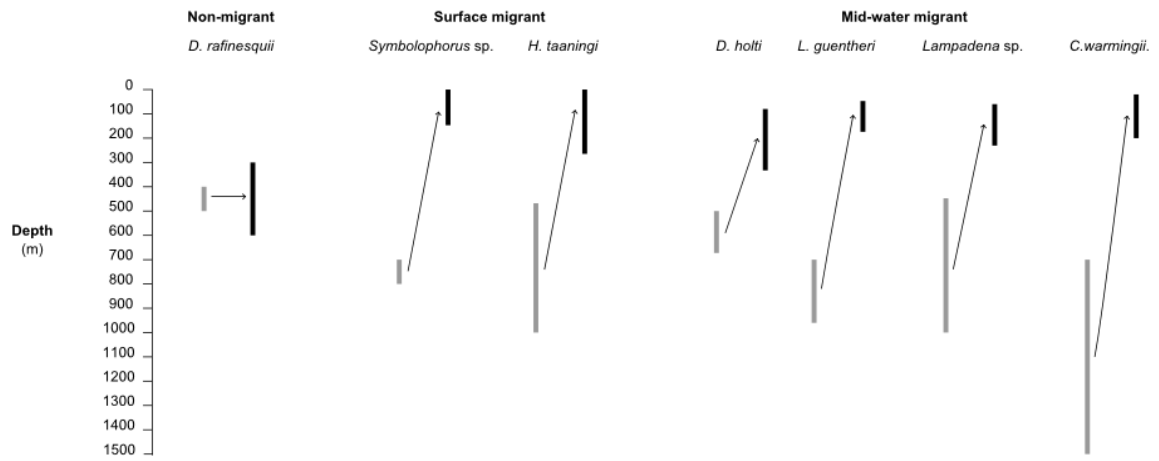

Figure 12 – Diagram showing DVM patterns and respective depths for the analysed species. Grey bars represent daytime depth distributions and black bars night-time depth. Depth data from Hulley (1989) and DVM data from Watanabe *et al*. (1999).

4.2.3. Phylogenetic relations

de Busserolles (2013) observed a phylogenetic relationship on RGCs specializations, but the sample size and the number of taxa used in the present study cannot be used to confirm such patterns. Nevertheless, the data presented here suggests that PRs specializations are interspecific. Streak-like specialized retinas only occured in species of the Myctophinae sub-family (*Symbolophorus* sp. and *H. taaningi*) while arches and rings only occurred in species of the Lampanyctinae sub-family (*D. holti*, *D. rafinesquii*, *Lampadena* sp., *L. guentheri* and *C.*

warmingii). In the same way, ring specializations were found in *Ceratoscopelus warmingii* and *Lepidophanes guentheri* which accord to Moser *et al.* (1984) are phylogenetically close. This shows that besides ecological parameters, such as biotic interactions, depth distributions, DVM patterns and light regimes, myctophids vision can also be phylogenetically constrained but once again, the data presented here must be analysed carefully, since this study only includes one individual in each of seven myctophid species.

5. Conclusion

All the analysed myctophid species revealed high visual sensitivity and low acuity, showing a visual adaptation to the mesopelagic dim and monochromatic light. Higher density and variations in rods than for RGCs support the fact that myctophids rely more on visual sensitivity than acuity. Even if some parameters do not vary much between species, some of them (*Symbolophorus* sp. and *Lampadena* sp.) seem to be more specialized for sensitivity to bioluminescence, while other (*H. taaningi* and *C. warmingii*) to the downwelling sunlight. This indicates that species are well adapted to these two types of light sources, which characterize the mesopelagic zone. The existence of different visual specializations for PRs and RGCs of the myctophids' retinas indicates that these fishes rely on vision for different ecological tasks.

6. References

Barnes, A.T. & J.F. Cage. 1974. The luminescence of lanternfish (Myctophidae): spontaneous activity and responses to mechanical, electrical and chemical stimulation. Journal of Experimental Marine Biology and Ecology. 15: 203-221.

Bergstad, O.A., Wik, Å.D. & Ø. Hildre. 2003. Predator-prey relationships and food source of the Skagerrak deep-water fish assemblage. Journal of Northwest Atlantic Fishery Science. 31: 165-180.

Bowmaker, J.K & H.-J. Wagner. 2004. Pineal organs of deep-sea fish: photopigments and structure. The Journal of Experimental Biology. 207: 2379-2387.

Bowmaker, J.K., Dartnall, H.J.A. & P.J. Herring. 1988. Longwave-sensitive visual pigments in some deep-sea fishes: segregation of "paired" rhodopsins and porphyropsins. Journal of Comparative Physiology. 163: 685-698.

Catul, V., Gauns, M. & P.K. Karuppasamy. 2011. A review on mesopelagic fishes belonging to family Myctophidae. Reviews.in Fish. Biology and Fisheries. 21: 339-354.

Cocker, J.E. 1978. Adaptations of deep sea fishes. Environmental Biology of Fishes. 3(4): 389-399.

Collin, S.P. & Pettigrew, J.D. 1989. Quantitative comparison of the limits on visual spatial resolution set by the ganglion cell layer in twelve species of reef teleosts. Brain, Behaviour and Evolution. 34: 184-192.

Collin, S.P., Llyod, D.J & H.-J. Wagner. 2000. Foveate vision on deep-sea teleosts: a comparison of primary visual and olfactory inputs. Philosophical Transactions of the Royal Society of London: Biological Sciences. 355: 1315-1320.

Crescitelli, F., McFall-Ngai, M. & J. Horwitz. 1985. The visual pigment sensitivity hypothesis: further evidence from fishes of varying habitats. Journal of Comparative Physiology. 157: 323-333.

de Busserolles, F. 2013. Myctophid vision: seeing and being seen in the mesopelagic zone. Ph.D. Thesis, The University of Western Australia, Crawley. 308 pp.

de Busserolles, F., Marshal, N.J. & S.P. Collin. 2014. The eyes of lanternfishes (Myctophidae, Teleostei): Novel ocular specializations for vision in dim light. Journal of Comparative Neurology. 552(7): 1618-1640.

Denton, E.J. & F.J. Warren. 1957. The photosensitive pigments in the retinae of deep-sea fish. Journal of the Marine Biological Association of the United Kingdom 36: 651-662.

Denton, E.J., Herring, P.J., Widder, E.A., Latz, M.F. & J.F. Case. 1985. The roles of filters in the photophores of oceanic animals and their relation to vision in the oceanic environment. Proceedings of the Royal Society: Biological Sciences. 225: 63-97.

Douglas, R.H., Partridge, J.C. & A.J. Hope. 1995. Visual and lenticular pigments in the eye of demersal deep-sea fishes. Journal of Comparative Physiology. 177: 111-122.

Douglas, R.H., Partridge, J.C. & N.J. Marshall. 1998. The eyes of deep-sea fish I: lens pigmentation, tapeta and visual pigments. Progress in Retinal and Eye Research. 17(4): 597-636.

Edwards, A.S. & P.J. Herring. 1977. Observations on the comparative morphology and operation of photogenic tissues of myctophid fishes. Marine Biology. 41: 59-70.

Evans, B.I. & R.D. Fernald. 1990. Metamorphosis and fish vision. Journal of Neurobiology. 23(7): 1037-1052.

Haddock, S.H.D., Moline, M.A. & J.F. Case. 2010. Bioluminescence in the sea. Annual Review of Marine Science. 2: 443-493.

Hasegawa, E.I., Sawada, K., Abe, K. Watanabe, K., Uchikawa, K., Okazaki, Y., Toyama, M. & R.H. Douglas. 2008. The visual pigments of a deep-sea myctophid fish *Myctophum nitidulum* Garman; an HPLC and spectroscopic description of a non-paired rhodopsin-porphyropsin system. Journal of Fish Biology. 72: 937-945.

Hope, A.J., Partridge, J.C., Dulai, K.S. & D.M. Hunt. 1997. Mechanisms of wavelength tuning in the rod opsins of deep-sea fishes. Proceedings of the Royal Society: Biological Sciences. 264: 155-163.

Hulley, P.A. 1989. Myctophidae. *In* Whitehead, P.J.P., Bauchot, M.-L., Hureau, J.-C., Nielsen, J. & E. Tortonese (Eds). Fishes of the North-eastern Atlantic and the Mediterranean (Vol. 1), United Kingdom. 429-483 pp.

Hulley, P. A. 1994. Lanternfishes. *In* Paxton, J. R. and Eschmeyer, W. N. (Eds.) Encyclopedia of fishes. Academic Press, San Diego. p. 127-128.

Hunt, D.M., Dulai, K.S., Partridge, J.C., Cottrill, P. & J.K. Bowmaker. 2001. The molecular basis for spectral tuning of rod visual pigments in the deep-sea fish. The Journal of Experimental Biology. 204: 3333-3344.

Johnsen, S., Widder, E.A. & C.D. Mobley. 2004. Propagation and perception of bioluminescence: factors affecting counterillumination as a cryptic strategy. The Biological Bulletin. 207: 1-16.

Johnsen, S. 2005. The red and the black: bioluminescence and the colour of animals in the deep-sea. Integrative & Comparative Biology. 45: 234-246.

Krönström, J & J. Mallefet. 2010. Evidence for a widespread involvement of NO in control of photogenesis in bioluminescent fish. Acta Zoologica. 91: 474-483.

Lythgoe, J.N. & J.C. Partridge. 1989. Visual pigments and the acquisition of visual information. The Journal of Experimental Biology. 146: 1-20.

Locket, N.A. 1980. Variation of architecture with size in the multiple-bank retina of a deep-sea teleost, *Chauliodus sloani*. Proceedings of the Royal Society: Biological Sciences. 208: 223-242.

McFall-Ngai, M., Crescitelli, F., Childress, J. & J. Horwitz. 1986. Patterns of pigmentation in the eye lens of the deep-sea hatchetfish, *Argyropelecus affinis* Garman. Journal of Comparative Physiology A.159: 791-800.

McNulty, J.A. 1976. A comparative study of the pineal complex in the deep-sea fishes *Bathylagus wesethi* and *Nezumia liolepis*. Cell and Tissue Research. 172: 205-225.

Mensinger, A.F. & J.F. Case. 1997. Luminescent proprieties of fishes from nearshore California basins. Journal of Experimental Marine Biology and Ecology. 210: 75-90.

Moser, H.G. & E.H. Ahlstrom. 1972. Development of the lanternfish, *Scopelopsis multipunctatus* Brauer 1906, with a discussion of its phylogenetic position in the family Myctophidae and its role in a proposed mechanism for the evolution of photophore patterns in lanternfishes. Fishery Bulletin. 70(3): 541-564.

Moser, H.G., Ahlstrom, E.H. & J.R. Paxton. 1984. Myctophidae: Development. *In* Moser, H.G., Richards, W.J., Cohen, D.M., Fahay, M.P., Kendall, Jr., A.W. & S.L. Richardson (Eds.). Ontogeny and systematics of fishes: based on an international symposium dedicated to the memory of Elbert Halvor Ahlstrom, Lawrence, United States of America. 218-239 pp.

Munk, O. 1977. The visual cells and retinal tapetum of the foveate deep-sea fish *Scopelosaurus lepidus* (Teleostei). Zoomorphologie. 87: 21-49.

Murphy, E. J., Watkins, J. L., Trathan, P. N., Reid, K., Meredith, M. P., Thorpe, S. E., Johnson, N. M., Clarke, A., Tarling, G.A., Collins, M.A., Forcada, J, Shreeve, R.S., Atkinson, A., Korb, R., Whitehouse, M.J., Ward, P., Rodhouse, P.G., Enderlein, P., Hirst, A.G., Martin, A.R., Hill, S.L., Staniland, I.J., Pond, D.W., Briggs, D.R., Cunningham, N.J. & A.H. Fleming. 2007. Spatial and temporal operation of the Scotia Sea ecosystem: a review of large-scale links in a krill centred food web. Philosophical Transactions of the Royal Society: Biological Sciences. 362: 113–148.

O'Day, W.T. & H.R. Fernandez. 1976. Vision in the Lanternfish *Stenobrachius leucopsarus* (Myctophidae). Marine Biology. 37: 187-195.

Owens, G.L., Rennison, D.J., Allison, W.T. & J.S. Taylor. 2012. In the four-eyed fish (*Anableps anableps*), the regions of the retina exposed to aquatic and aerial light do not express the same set of opsin genes. Biology Letters. 8: 86-89.

Pankhurst, N.W. 1987. Intra- and interspecific changes in retinal morphology among mesopelagic and demersal teleosts from the slope waters of New Zealand. Environmental Biology of Fishes. 19(4): 269-280.

Pante, E. & B. Simon-Bouhet. 2013. Marmap: A package for importing, plotting and analysing bathymetric and topographic data in R. PLoS ONE. 8(9), e73051. (doi:10.1371/journal.pone.0073051).

Partridge, J.C., Archer, S.N. & J.N. Lythgoe. 1988. Visual pigments in the individual rods of deep-sea fishes. Journal of Comparative Physiology. 16: 543-550.

Partridge, J.C., Shand, J., Archer, S.N., Lythgoe, J.N. & W.A.H.M. van Groningen-Luyben. 1989. Interspecific variation in the visual pigments of deep-sea fish. Journal of Comparative Physiology. 164: 513-529.

Rasband, W. S. 1997–2014. ImageJ. U. S. National Institutes of Health, Bethesda, MD. Available at http://imagej.nih.gov/ij/.

Robinson, C., Steinberg, D. K., Anderson, T. R., Arístegui, J., Carlson, C. A., Frost, J. R., Ghiglione, J.-F., Hernández-León, S., Jackson, G. A., Koppelmann, R., Quéguiner, B., Ragueneau, O., Rassoulzadegan, F., Robison, B. H., Tamburini, C., Tanaka, T., Wishner, K. F. & Zhang, J. 2010. Mesopelagic zone ecology and biogeochemistry – a synthesis. Deep-Sea Research II. 57: 1504–1518.

Sabatés, A., Bozzano, A. & I. Vallvey. 2003. Feeding pattern and the visual light environment in myctophid fish larvae. Journal of Fish Biology. 63: 1476-1490.

Salvanes, A.G.V & J.B. Kristoffersen. 2001. Mesopelagic fishes. *In* Steele, J.H., Hoagland, P.A., Tyack, P., Schumacher, M., Trask, R.P. & R.A. Weller (Eds.). Encyclopedia of ocean sciences (Vol. 3). University of Bergen, Bergen, Norway. Academic Press.

Shreeve, R.S., Collins, M. A., Tarling, G.A., Main, C.E., Ward, P. & N.M. Johnston. 2009. Feeding ecology of myctophid fish in the northern Scotia Sea. Marine Ecology Progress Series. 386: 221-236.

Somiya, H. 1982. "Yellow lens" eyes of a stomiatoid deep-sea fish, *Malacosteus niger*. Proceedings of the Royal Society: Biological Sciences. 215: 481-489.

Sutton, T.T. 2013. Vertical ecology of the pelagic ocean: classical patterns and new perspectives. Journal of Fish Biology. 83: 1508-1527.

Toyama, M, Hironaka, M., Yamahama, Y., Horiguchi, H., Tsukada, O., Uto, N., Ueno, Y., Tokunaga, F., Seno, K. & T. Hariyama. 2008. Presence of rhodopsin and porphyropsin in the eyes of 164 fishes, representing marine, diadromous, coastal and freshwater species – a qualitative and comparative study. photochemistry and photobiology. 84: 996-1002.

Trueman, C.N., Johnston, G., O'Hea, B. and MacKenzie, K.M. 2014. Trophic interactions of fish communities at midwater depths enhance long-term carbon storage and benthic production on continental slopes. *Proceedings of the Royal Society B Biological Sciences*, 281(1787), 20140669. (doi:10.1098/rspb.2014.0669).

Turner, J.R., White, E.M., Collins, M.A., Partridge, J.C. & R.H., Douglas. 2009. Vision in lanternfish (Myctophidae): Adaptations for viewing bioluminescence in the deep-sea. Deep-Sea Research Part I. 1003-1017.

Vieira, R.P.S. 2011. *Estrutura populacional de* Electrona antarctica (Günther, 1878) e Gymnoscopelus braueri (Lönnberg, 1905) *no Mar da Scotia (Oceano Antárctico)*. MSc Thesis, University of Algarve, Faro. 109 pp-

Wagner, H.-J. 2002. Sensory brain areas in three families of deep-sea fish (slickheads, eels and grenadiers): comparison of mesopelagic and demersal species. Marine Biology. 141: 807-817.

Wagner, H.-J., Fröhlich, E., Negishi, K. & S.P. Collin. 1998. The eyes of deep-sea fish II. functional morphology of the retina. Progress in Retinal and Eye Research. 17(4): 637-685.

Warrant, E.J. & N.A. Locket. 2004. Vision in the deep sea. Biological Reviews. 79(3): 671-712.

Watanabe, H., Moku, M. Kawaguchi, K. Ishimaru, K. & A. Ohno. 1999. Diel vertical migration of myctophid fishes (Family Myctophidae) in the transitional waters of the western North Pacific. Fisheries Oceanography. 8(2): 115-127.

Yakir, L.G, Sutton, T.T & S. Johnsen. 2013. Visual acuity in pelagic fishes and molluscs. Vision Research. 92: 1-9.

Yokoyama, S. & R. Yokoyama. 1996. Adaptive evolution of photoreceptors and visual pigments in vertebrates. Annual Reviews of Ecology, Evolution and Systematics. 27: 543-567.

Young, R.E., Roper, C.F.E. & J.F. Walters. 1979. Eyes and extraocular photoreceptors in midwater cephalopods and fishes: their roles in detecting down-welling light for counterillumination. Marine Biology. 51: 371-380.

Appendix I. Retinal wholemounting technique protocol for myctophids[1]

Material

- Callipers
- Desiccator
- Digital camera (Fujifilm FinePixZ10df)
- Dissection microscope (Leica MZ6) and respective illuminator (Leica L2)
- Dissection microscope (Leica S8AP0 linked to a Leica MC170 HD camera)
- Fine forceps
- Forceps
- Fume hood
- Immersion oil
- Latex gloves
- Microknife
- Mini-scissors
- Nail varnish
- Optical Microscope (Nikon Labophot-2) and attached digital camera (Nikon DS-Fi1)
- Paintbrush
- Paper towel
- Plastic Pasteur pipettes
- Petri dish
- Scalpel
- Slides and cover slips
- Staining rack with respective glass staining dish
- Universal glue
- Xilol

[1] Adapted from Ullman *et al.* (2011) and De Busserolles (2013).

Reagents

- Paraformaldehyde
- 0,1M phosphate buffer solution (PBS)[2] (pH 7.4 at 4ºC)
- 4% paraformaldehyde in 0.1 M phosphate buffer
- Ethanol (100, 90, 70 and 20%)
- Glycerol (100%)
- Histoclear
- Gatenby's solution:
    - Heat 1.5 g of gelatin in 7 ml of glacial acetic acid until the gelatin dissolves;
    - Prepare 2 ml of distilled water and 0.1 g of chromium potassium sulphate;.
    - Mix the two solutions.
- 0,1 Cresyl violet stain (pH 3,7 in acetate buffer): 0,4g of Cresyl violet, 10ml of glacial acetic acid, 10ml of 1M sodium acetate and 380ml of distilled water (filter before use).
- Differentiation solution: 900 ml of 96% ethanol and 1 ml of glacial acetic acid (filter before use).

Software

- GIMP 2.8.10 , developed by The GIMP Development Team
- ImageJ 1.47V, developed by National Institute of Health of the United States of America
- NIS-Elements D2.30, developed by Nikon

[2] It was used a 100x dilution of a 10M commercial PBS solution (PBS without Ca and Mg (10x,) 1000ml, BioWhittaker Europe).

I. Eye orientation and enucleation

1. Before enucleation external characteristics[3] of the eye were annotated, and a digital photograph taken (Fig. 1). Photographs were taken to ensure the correct eye orientation.

Figure 1 –*Lepidophanes guentheri* showing the left eye before enucleation.

2. While holding the fish head with the fine forceps, the eye was gently rotated forward and the conjunctiva (Fig. 2) cut with a microknife.

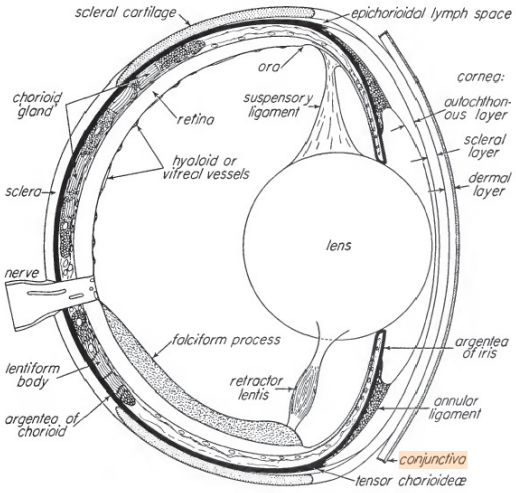

Figure 2 – Diagram of eyeball anatomy, showing the conjunctiva. Adapted from De Busserolles, 2013.

3. The eyeball was gently pulled out from the orbit and the adipose and muscle tissues cut, with mini-scissor. The optical nerve was gently cut, leaving a small portion of it.

[3] Mainly, differences in pigmentation of the iris and aphakic gap.

4. Digital photographs of the enucleated eye were taken and eye dimensions measurement (Fig. 3).

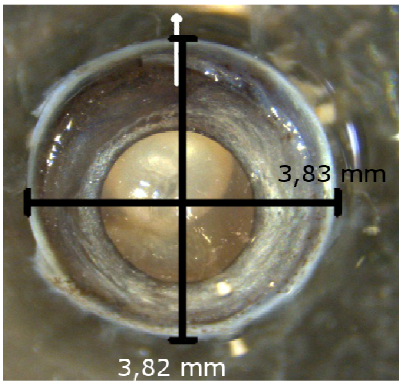

Figure 3 – Enucleated left eye of *Lepidophanes guentheri* showing the dorsoventral and rostrocaudal eye diameters. The white arrow points the dorsal orientation of the eye.

II. Opening the eye and cornea and lens extraction

1. The eye was placed with the cornea side up. With fine forceps, the cornea was gently hold to show a small fold, in order to easily be cut with mini-scissors.
2. The cornea was cut along the edge with mini-scissors, slowly to avoid damaging the iris, once its pigmentation is the main orientation reference. Lens was gently pulled out from the orbit and the lens muscles cut with miniforceps
3. Digital photographs of the lens were taken to measure the diameter of the lens (Fig. 4). Then, the lens was kept in PBS buffer.

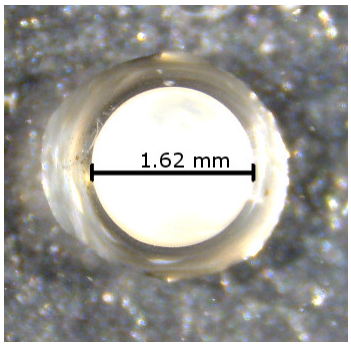

Figure 4 – Lens diameter measured from a digital photograph of a lens extracted from *Lepidophanes guentheri*.

III. Retinal fixation[4]

1. The entire eyecup was submerged in paraformaldehyde with phosphate buffer for 60-120 minutes. Fixation solution should be 5 times the eyecup volume, at least. When manoeuvring the eyecup, special care was taken to hold it from the remaining muscles or optic nerve, with fine forceps.
2. The eyecup was removed from the fixation solution and washed in PBS, for approximately 1 minute.

IV. Retinal extraction

1. The eyecup was placed in a Petri dish with chilled PBS under the dissection microscope.
2. Using fine forceps and mini-scissors, the iris was gently cut along the edge, with the exception of the dorsal part, for orientation purposes.
3. The vitreous humour (and some cornea and iris remains, eventually) was gently pulled with fine forceps and cut with the mini-scissors. As this is a transparent tissue and it is located near the retina, it was not entirely removed, to avoid to damaging the retina.
4. For orientation purposes, with the mini-scissors. the dorsal position of the retina was gently marked, with a deep radial cut, about 2/3 of its radius, with care to do not cut near the optic nerve. This cut helps to open the sclera.
5. The eyeball was turned with the dorsal side up, to facilitate the access to the scleral cut made right before.
6. The sclera was cut all around, perpendicularly to the radial cut. The cut has to be done really gently, since the scissors can get in contact with the retina, damaging it. As the cut goes through, the sclera and choroidal tissue detach from the retina by itself, so the detached tissue can be gently cut and removed.
7. Sclera was removed with care to avoid damaging the retina.
8. Using a paintbrush, the remaining choroid and retinal pigmented epithelium (RPE) were removed. When small portions of the RPE were hard to detach from the retinal periphery, it was not removed to avoid damaging the retina.
9. The remaining optic nerve was gently removed and a digital photograph was taken (Fig. 5A).

[4] For teleosts, Ullmann et al. (2011) and De Busserolles, (2013) recommend retinal fixation prior to removal

10. Finally, with the mini-scissors, 3-4 clean radial cuts about 2/3 of the retinal radius diameter were done, to allow the retina to be flattened without ripping it. A digital photograph was taken (Fig. 5B). The radial cuts can be done only when placed the retina on the slide, since the retina is more fragile with the cuts

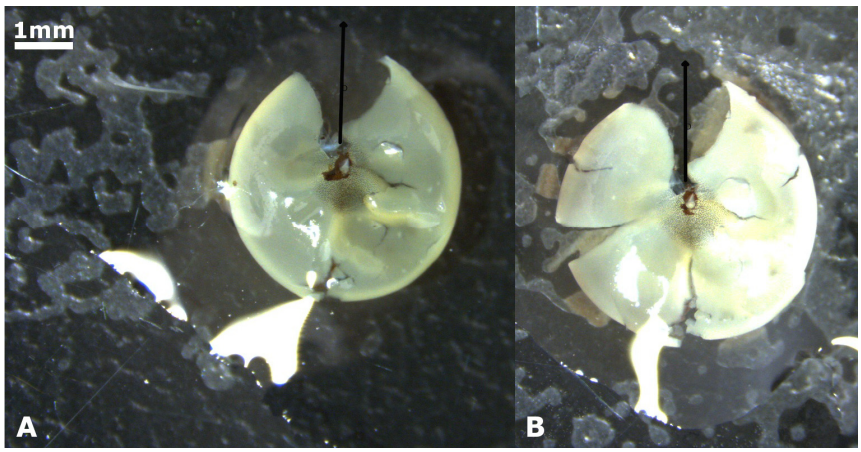

Figure 5 – Extracted retina from the left eye of *Lepidophanes guentheri*, showing A) pre- and B) post radial cuts. Arrows indicates the dorsal side of the eye.

V. Cover slips and slides preparation

When possible, new cover slips were used, when recycled slides were used, they were cleaned with ethanol 96%.

For RGCs mountings, gelatinized slides are required. For this purpose, cover one side of the slide with Gatenby's solution 2 or 3 times. To ensure the slides were dry between coatings, they were placed into an oven at 37ºC. After the last coating, gelatinized slides were kept at the oven for minimum 8 hours.

To avoid any damage to the retina while examining it, a spacer was created from paper strips and nail varnish, as glue. As the spacer should be slightly thicker than the retina, two paper layers were used (Fig. 6). This technique was only used for RGCs permanent mounting, since PRs mountings were temporary, only a few quantity of glue was used between the edges of the slide and cover slip. Also, with dry glue it is easy to take off the cover slip without brake it, avoiding glass fragments on the retina's surface.

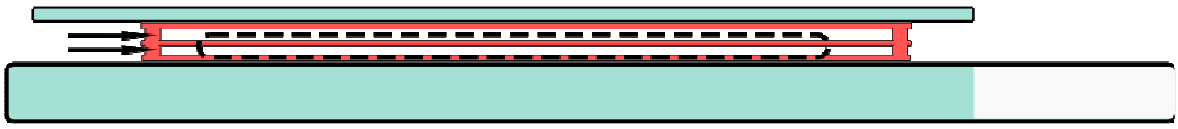

Figure 6 – Scheme of the RGCs mounting showing the spacer and the retina inside. Red lines represent the layers of nail varnish and the arrows point to the two paper strips layers (white bands) in it. Dashed lines represent the retina inside the mounting.

VI. Retinal wholemounting

Since RGCs mounting involve gelatinized slides and staining procedures, for visualization of the neural cells on the same retina, PRs were examined before. For PRs observation, the scleral side of the retina has to be upwards, while for RGCs must be observed the vitreal side.

The extracted retina was floated onto a non-gelatinized slide. This step presented more difficulties, because the retina can be easily damaged. In order to facilitate the transferring process, the Petri dish used for retinal extraction was filled with PBS, the slide was placed in it, and the retina was gently carried to the centre of the slide, scleral side up. Then, the slide was taken from the PBS and the buffer excess absorbed with a paper towel, with care to avoid touching the retina. A paintbrush was used to help flatten the retina, avoiding folds.

VII. Retinal cell visualization

VII.1. Photoreceptors

1. One or two drops of glycerol were placed onto the mounted retina (Fig. 7) in order to obtain a 50/50 glycerol/buffer.
2. PRs were observed under the 100x objective of an optical microscope (Fig. 8). A digital photograph of the mounted retina was taken after the observation of PRs. Because the retinas may be squashed and suffer small rips during the observation under the 100x objective, a post-observation photograph ensures a more accurate map.

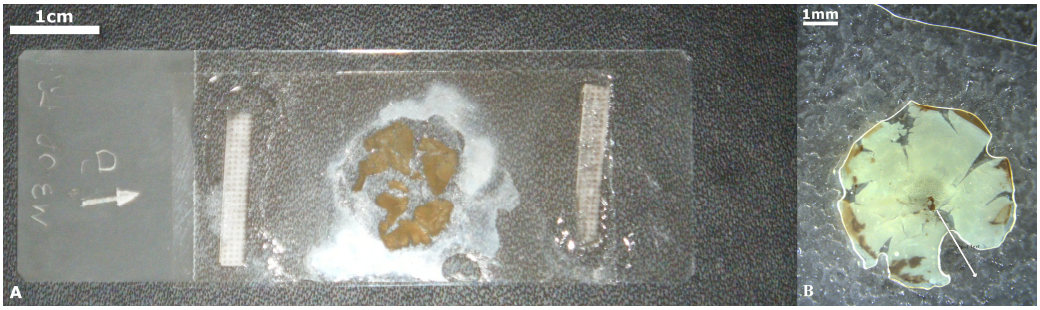

Figure 7 – Digital photographs of PRs' mountings from myctophids. A) Full view of a *Symbolophorus* sp. mounting; B) Close look of a mounted retina from *Lepidophanes guentheri*. Arrow indicates the dorsal side of the eye.

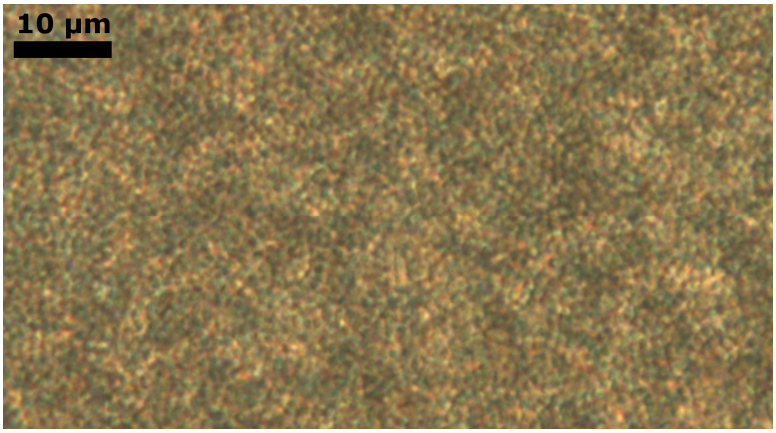

Figure 8 – Digital photograph of PRs from a myctophid retina, observed under 100x objective of an optical microscope.

VII.2. Retinal ganglion cells

1. Using a scalpel, some pressure was gently made onto the glue to detach the cover slip from the slide. Once the cover slip was removed, the slide was gently scraped with a scalpel and cleaned with paper towel, to remove the remaining glue.
2. Some drops of PBS were placed on the retina to remove the glycerol.
3. The retina was placed on a freshly gelatinized slide, with the vitreal side facing up. For this purpose, the gelatinized slide was placed on the retina and a small pressure was gently applied. Then, the slides were turned upside-down and the non-gelatinized slide was slowly pulled up, in order to detach the retina without fragmenting the tissue. With the scleral side facing up, for PRs observation, this step places it directly with the vitreal side up, ready for the RGCs observation. A paintbrush was used to gently flatten the retina on the gelatinized slide, to avoid folds, and photographs were taken (Fig. 9A).

4. In order to dry the retina on the gelatinized slide, it was placed horizontally, on a moist paper towel inside a Petri dish in the desiccator. The desiccator lid was first placed with just a little gap to avoid condensation, and it was gently opened every 3 or 4 days until the retina present a dry aspect (Fig. 9B).

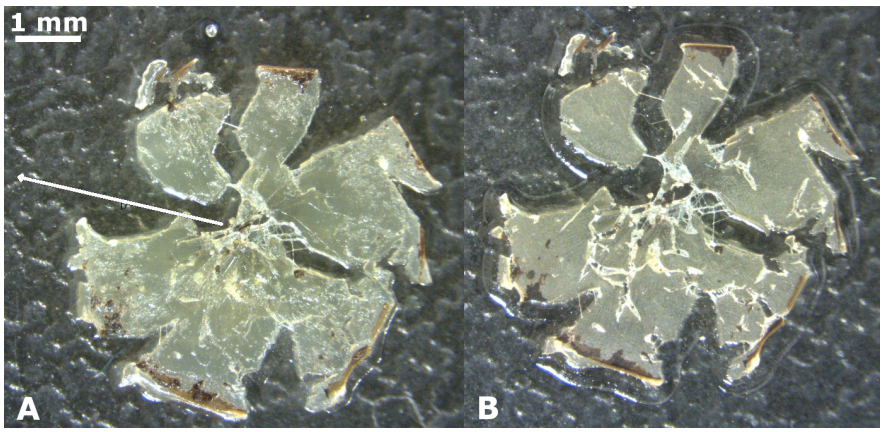

Figure 9 – Digital photographs of the left retina of a *Lepidophanes guentheri*. A) Before drying; and B) after drying. Arrow indicates the dorsal side of the eye.

5. The retina was stained with 0,1% Cresyl violet, following procedure in Table I:

Table I – Procedure for 0,1 Cresyl violet staining. Adapted from Ullmann et al. (2011).

Stage	Staining tray	Time	Purpose
1	Histoclear	15 min	clearing agent
2	100% ethanol	3 min	defatting
3	90% ethanol	2 min	rehydration
4	70% ethanol	2 min	rehydration
5	20% ethanol	1 min	rehydration
6	Distilled water	2 min	rehydration
7	0,1% Cresyl violet	20 min	staining
8	Distilled water	quick rinse	rehydration
9	20% ethanol	30 s	rehydration
10	70% ethanol	30 s	rehydration
11	90% ethanol	30 s	rehydration
12	Differentiation solution	1 min	differentiation
13	100% ethanol	1,5 min	dehydration
14	Histoclear	3 min	clearing agent

6. The staining solution excess was removed with paper towel, and the slide placed on paper towel for, at least, 30 minutes, to ensure the remaining histoclear drying.

7. The mounting for RGCs (Fig. 10A) was done as explained in the Section V. The nail varnish was dry from layer to layer of the spacer and before the mounting media application. For this purpose, only one drop of glycerol was placed on the retina. Then, nail varnish was gently applied on the spacer, allowing it to glue the cover slip. Finally, the cover slip was slowly placed on the spacer (Fig. 10B).

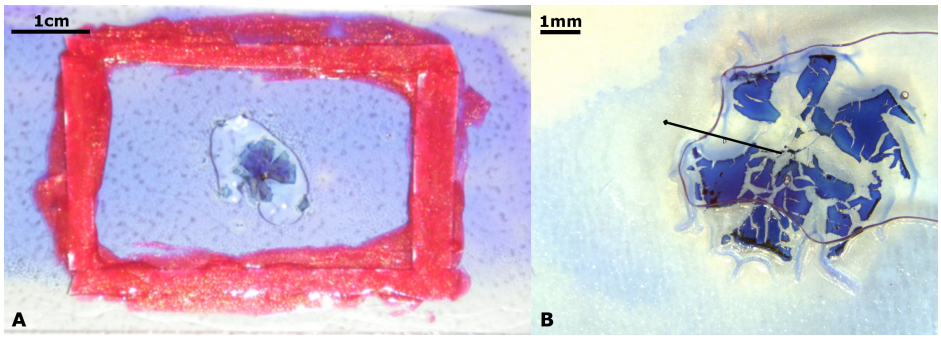

Figure 10 - Digital photographs of RGCs' mountings. A) Full view of a *Diaphus holti*. mounting; B) Close look of a mounted retina from *Lepidophanes guentheri*. Arrow indicates the dorsal side of the eye.

8. The retina was observed under the 40x objective of an optical microscope, to avoid the retina to get squashed and ripped during the observation.

VIII. Mapping retinal cell distributions

VIII.1. Photoreceptors

1. Coordinates of the vertical and horizontal edges were annotated and a value was defined for the distance between sampling areas (SAs), in order to obtain more than 200[5] SAs in any single retina.
2. The retinas was then scanned from the top to the bottom by horizontal transects and from left to right side in each SA. Horizontal and vertical coordinates were taken for each transect and for each SA, respectively. Transects were labelled by a capital letter (in alphabetic order from the top to the bottom) and the SAs by numbers for each transects.
3. Digital photographs were taken for each SA.Several photographs were taken per SA in order to focus different parts of the analysed area, as the retina present an irregular surface when mounted.

[5] Value stablished by Ullmann et al. (2011) and de Busserolles, (2013).

VIII.2. Retinal ganglion cells

Contrary to PRs, RGCs are distinguishable with the 40x objective, so this objective was used for these neural cells' observation. Nevertheless, the procedure for RGCs mapping, was similar to the PRs. Since the amplification used was lower for RGCs than PRs and the total SAs number rarely approached 200, the entire retinas was scanned.

IX. Topographic map[6]

1. Digital photographs of the retinas mountings were used to create the topographic maps (Fig. 11A).
2. Vertical and horizontal grids were added to the image and aligned with the respective axis edges of the outline.
3. To create a preliminary map, 150 SAs were evenly selected and labelled in the image, aligned to the horizontal grid within each transect, and aligned with the vertical grid by transect (Fig 11B).
4. The cells counting procedure was the same for PRs and RGCs, but for RGCs, ACs were simultaneously counted. One photograph per previously selected SA was chosen and a 100 μm^2 grid applied. Five grid squares were chosen as counting replicates, from which a final average was calculated to represent the cell density for each selected SA (cells/100 μm^2).
5. The cell densities for the selected SAs calculated in the step above replaced the respective SAs labels on the map (Fig. 11C).
6. The cell densities were replaced by a numeric scale (Fig. 11D) that corresponds to the colour gradient of the topographic map (Fig. 11E).
7. The layout obtained represents a preliminary map, as stated in (5). For the final map, 50 non-selected SAs were included within the high density zones of the preliminary map. This aimed to achieve a greater definition by subsampling higher cell density areas of the retina.
8. The final topographic map (Fig. 11F) should include: 1. retinal outline; 2. iso-density lines or colour gradation; 3. natural landmarks; 4. retinal orientation; and 5. scale bar.

[6] For steps (e) (h) (i), ImageJ 1.47V was used. The rest was developed with GIMP 2.8.10.

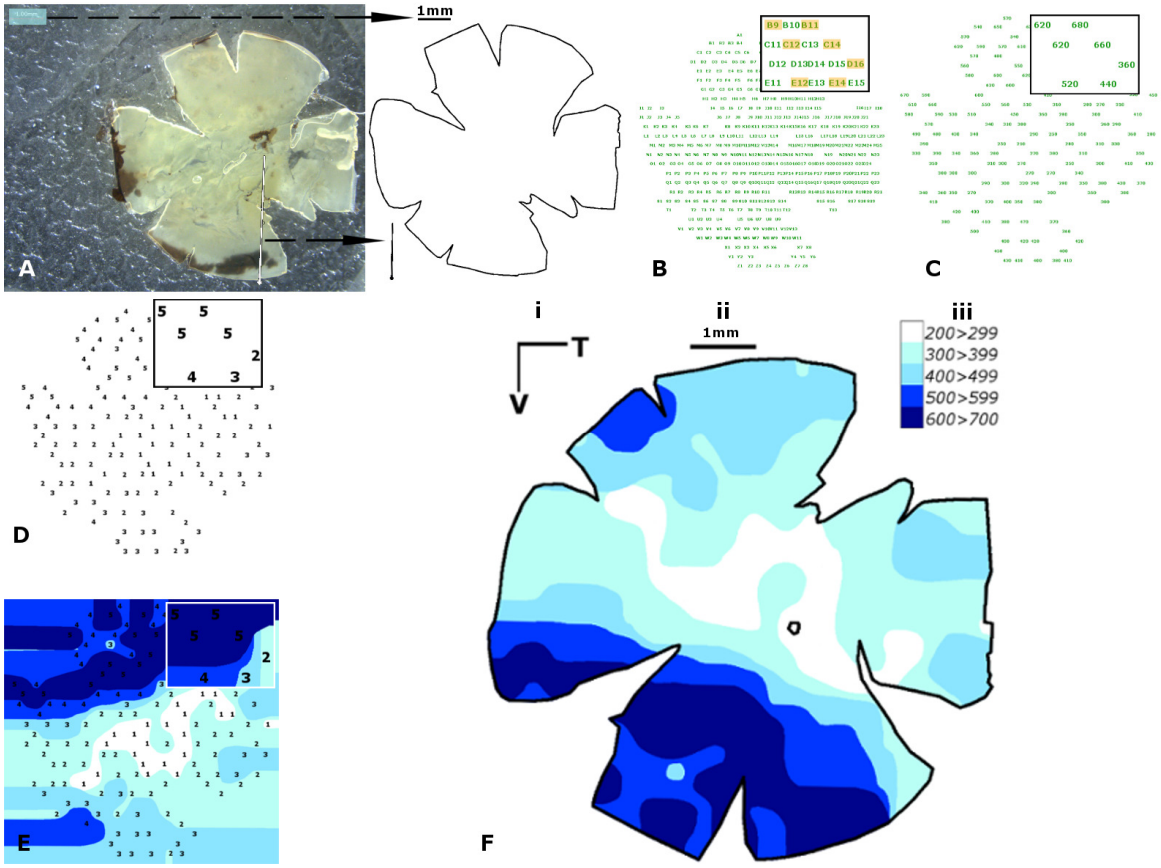

Figure 11 – Scheme representing the procedure of density topographic mapping for *Hygophum taaningi*. A) Creating the outlier, scale, and eye orientation from a retina's scaled photograph; B) adding the SAs; C)replacing the SAs with respective cell density values; D) replacing the cell density values with the respective numeric scale values; E)grouping numeric scale values and filling the groups with respective colour gradation; F) topographic map with outline, confirmed eye orientation (T= temporal, V= ventral), scale (ii), and legend corresponding colour gradation scale to numeric scale of cells' density (x 10^3 cells.mm^{-2}). A) Original photograph scale highlighted; white and black arrows indicate the dorsal side of the eye; dashed lines represent extrapolation. B) Selected SAs highlighted. The small boxes in B), C), D) and E) represent amplifications of the underneath part of the maps.

Appendix II. Methodological issues

The wholemounting technique protocol used in this study was primarily based on Ullmann *et al*. (2011), who presented a general procedure for vertebrates. The observation of other retinas from different fish species (not included in this study) revealed that myctophids possess a singular retina, and allowed a subsequent optimization of the protocol. In this way, some factors varied between retinal treatments for different specimens (Table I). For future observations, the transition of the retinas from the PRs mounting slide to the gelatinized one should be done by floating the retinas in PBS instead of turning slides upside-down (see Appendix I), in order to avoid a possible displacement of the retinas. Another further improvement should be the use of a permanent mounting media instead of glycerol, since this solution clears the neural cells, making them harder to distinguish within a month from the mounting process. The stress caused by the fishing or the post-mortem condition of the retinae might contribute to the difficulties found during the analysis. Additionally, fishes with smaller eyes possess smaller neural cells, and more difficult to distinguish. Some methodological implications seem to be related with the difficulty to analyse the neural cells: 1) the specimens were already fixed in 4% paraformaldehyde (see Material and methods, page 14) when retinas were collected. In the laboratory, an additional retinal fixation was done (see Appendix I, section III), which could have contributed to the brighter neural cells, making it difficult to distinguish; 2) a spacer should have been used to observe PRs, in order to avoid cells to squash, which makes it harder to identify these neurons; 3) retinas were not washed and incubated with PBS after PRs observations to remove all the remaining glue from the mountings, probably, affecting the staining conditions and, consequently, making RGCs difficult to distinguish.

Damaged retinas (see Results) seem to limit the analyses of neural cells, because RGCs specializations were not always easy to distinguish (Fig. 1), which could have cause miscounting in some retinas (e.g. *Symbolophorus* sp. and *Lepidophanes guentheri*). However, the reason for the neglected condition does not seem to be related with sampling, maintenance or methodology. Ullmann *et al*. (2011) suggested that the number of cells in the retinal periphery may lead to an overestimation, due to the relatively thin retinal periphery and the radial cuts and shrinkage of the retina while treated for RGCs observation. As observed by Collin & Pettigrew (1989), difficulty in distinguish ACs from RGCs might be a problem, and it could lead to an overestimation of RGCs.

Moreover, due to problems already mentioned, most retinas were damaged, which made difficult to identify and count RGCs, contributing to differences in results. The results obtained in this study differ from those obtained by de Busserolles (2013), most probably due to an observation bias that led to the overestimation of cells density values, especially for RGCs.

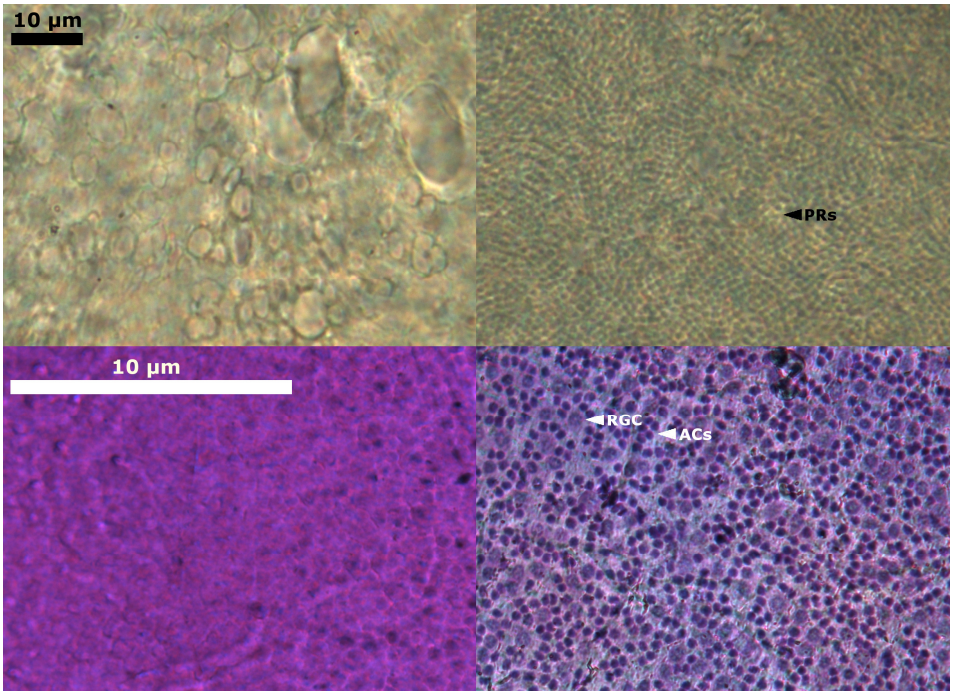

Figure 1 – Photographs of degraded and non-degraded retinas, showing the distinguishability of neural cells. A) PRs photographed under a 100x objective from a degraded retinas of *L. guentheri*; B) PRs photographed under a 100x objective from a non-degraded retinas of *C.* warmingii; C) ACs and RGCs photographed under a 40x objective from a degraded retinas of *L. guentheri*; D) ACs and RGCs photographed under a 40x objective from a degraded retinas of *C.* warmingii. White scale bar for PRs images and black one for ACs/RGCs ones.

Table I - Differences in retinal methodologies for wholemount analyses. (1) Sclera showing a little rip, exposing the rods; (2) both eyes with degraded retinae; (3) gelatinization in relation to drying; (4) Slide's dipping time at step 5 of retinal staining (see Table 1 of Appendix I). PRs=photoreceptors, ACs=amacrine cells, RGCs=retinal ganglion cells.

Species	Eye	Cell type mapping	Retinal fixation (hours)	Gelatinization conditions			Retina drying			Retina staining (4)
				Coats	Slides drying (heater time and temperature)	Gelatinization (3)	Recipient	Moist papper	Drying time (days)	(min)
Diaphus holti	Left	PRs	2							
	Right	RGCs/ACs	2	3	<1 hour at 37ºC	Before	Dissecator	Yes	21	2
D.iaphus rafinesquii	Left (1)	PRs	2							
	Right	RGCs/ACs	1	3	<1 hour at 37ºC	Before	Dissecator	Yes	21	2
Symbolophorus sp. (2)	Left	All	1.5	2	8 hours at 37ºC	After	Closed Petri dish in dissecator	No	4	1
Lampadena sp.	Left (1)	RGCs/ACs	2	2	8 hours at 50ºC	Before	Closed Petri dish in dissecator	Yes	12	1
	Right	PRs	2							
Hygophum taaningi	Left	All	2	2	8 hours at 37ºC	Before	Closed Petri dish in dissecator	Yes	3	1
Lepidophanes guentheri (2)	Left	RGCs/ACs	2	2	8 hours at 37ºC	Before	Closed Petri dish in dissecator	Yes	3	1
	Right	PRs	2							
Ceratoscopelus warmingii	Right	All	2	2	8 hours at 37ºC	After	Dissecator	No	4	1